1

Thermodynamic Properties of Ionic Liquids - Measurements and Predictions -

Zhi-Cheng Tan, Urs Welz-Biermann, Pei-Fang Yan,
Qing-Shan Liu and Da-Wei Fang
China Ionic Liquid Laboratory and Thermochemistry Laboratory
Dalian Institute of Chemical Physics, Chinese Academy of Sciences, Dalian 116023, China

1. Introduction

Research of ionic liquids (ILs) is one of the most rapidly growing fields in the past years, focusing on the ultimate aim of large scale industrial applications. Due to their unique tunable properties, such as negligible vapor pressure at room temperature, stable liquid phase over a wide temperature range and thermal stability at high temperatures, ionic liquids are creating an continuously growing interest to use them in synthesis and catalysis as well as extraction processes for the reduction of the amount of volatile organic solvents (VOSs) used in industry.

For the general understanding of these materials it is of importance to develop characterization techniques to determine their thermodynamic and physicochemical properties as well as predict properties of unknown Ionic Liquids to optimize their performance and to increase their potential future application areas.

Our laboratory in cooperation with several national and international academic and industrial partners is contributing to these efforts by the establishment of various dedicated characterization techniques (like activity coefficient measurements using GC technology) as well as determination of thermodynamic and physicochemical properties from a continuously growing portfolio of (functionalized) ionic liquids. Based on the received property data we published several papers related to the adjacent prediction of properties (like molar enthalpy of vaporization, parachor, interstice volume, interstice fractions, thermal expansion coefficient, standard entropy etc.). Additionally our laboratory created and launched a new most comprehensive Ionic Liquid property data base--delph-IL.(www.delphil.net). This fast growing collections of IL data will support researchers in the field to find and evaluate potential materials for their applications and hence decrease the time for new developments.

In this chapter we introduce the following techniques, summarize recent published results completed by our own investigations:

1. Activity coefficient measurements using GC technique,
2. Thermodynamic properties determined by adiabatic calorimetry and thermal analysis (DSC, TG-DTG).
3. Estimation and prediction of physicochemical properties of ILs based on experimental density and surface tension data.

1.1 Activity coefficient measurements using GC technique

For the use of Ionic Liquids as solvents it is very important to know about their interaction with different solutes. Activity coefficients at infinite dilution of a solute i(γ_i^∞) can be used to quantify the volatility of the solute as well as to provide information on the intermolecular energy between solvent and solute. Values of γ_i^∞ are also important for evaluating the potential uses of ILs in liquid-liquid extraction and extractive distillation. Since ILs have a negligible vapor pressure, the gas-liquid chromatography (GLC) using the ionic liquid as stationary phase, is the most suitable method for measuring activity coefficients at infinite dilution γ_i^∞.

A large number of studies on the activity coefficients at infinite dilution γ_i^∞ of organic solvents in different ILs have been reported in the past decade . In this section, we first introduce the experimental techniques used to measure the activity coefficients at infinite dilution, γ_i^∞; then describe our results of γ_i^∞ and compare them with literature data. Most results of these studies have been published since 2000. Finally, we dicuss the separation problems of hexane/benzene and cyclohexane/benzene by use of Ils based on the results of γ_i^∞.

1.2 Thermodynamic properties determined by adiabatic calorimetry and thermal analysis techniques (DSC and TG-DTG)

Thermodynamic properties of ionic liquids, such as heat capacity $C_{p,m}$, glass transition temperature T_g, melting temperature T_m, thermal decomposition temperature T_d, enthalpy and entropy of phase transitions are important data for the basic understanding of these materials and their application in academia and industry. These thermodynamic properties can be determined using adiabatic calorimetry and thermal analysis techniques (DSC, TG-DTG).

Our laboratory in cooperation with the thermochemistry laboratory at the Dalian Institute of Chemical Physics has a long history in the development and set up of specialized adiabatic calorimetric apparatus and the determination of the above listed thermodynamic properties of Ionic Liquids.

In this section, we introduce the required experimental techniques, the specific adiabatic calorimeter established in our laboratory, and describe our recently published results of thermodynamic property measurements for some typic ionic liquids.

1.3 Estimation and prediction of physicochemical properties of ILs based on experimental density and surface tension data.

More and more publications have reported the physicochemical properties of some ILs, but the overall amount of property data measured by experimental methods are still not fulfilling the requirements for their broad application, especially, due to the lack of data of IL homologues which would be helpful to improve the selection of more appropriate test candidates for different applications. A recently developed technical approach- based on the experimental data of densities and surface tensions of small number of ionic liquids - enables estimation and prediction of density, surface tension, molecular volume, molar volume, parachor, interstice volume, interstice fractions, thermal expansion coefficient, standard entropy, lattice energy and molar enthalpy of vaporization of their homologues.

In this section, we introduce the theoretical models for the prediction of additional physicochemical property data and describe our recently published results for three imidazolium-based ionic liquid homologues, [$C_n$mim][$EtSO_4$], [$C_n$mim][$OcSO_4$] and [$C_n$mim][NTf_2] (n=1-6).

2. Activity coefficient measurements using GC technique

2.1 Introduction

Ionic Liquids (ILs) are often called designer solvents or task specific ionic liquids (TSILs) because of their possible tailoring to fulfil technological demands of various applications. IL properties can be significantly adjusted by tailoring their anion and/or cation structures.[1] Due to their unique properties such as nonflammability, wide liquid range, stability at high temperatures, and negligible vapor pressure, ionic liquids created interest to use them in separation process as potential green replacement for conventional volatile, flammable and toxic organic solvents. Therefore it is very important to know their interaction with different solutes. Activity coefficients at infinite dilution of a solute i (γ_i^∞) can be used to quantify the volatility of the solute as well as to provide information on the intermolecular energy between solvent and solute.[2,3]

Since ILs have a negligible vapor pressure, the gas-liquid chromatography (GLC) using the ionic liquid as stationary phase is the most suitable method for measuring activity coefficients at infinite dilution γ_i^∞. Experimental γ_i^∞ data provide useful information about the interaction between the solvent (IL) and solute. Disubstituted imidazolium based ionic liquids are a class of very promising extraction and separation reagents, being reported in various publications. Most of this research work is based on anions like $[BF_4]^-$,[4-8] $[PF_6]^-$,[9] $[N(CF_3SO_2)_2]^-$,[10-14] $[Br]^-$,[15] $[Cl]^-$,[16] $[CF_3SO_3]^-$,[17-19] $[SCN]^-$,[20,21] $[MDEGSO_4]^-$,[22] $[FeCl_4]^-$,[23] and $[CoBr_4]^-$.[24] In separation processes property of the extractant is very important, namely its selectivity S_{ij}^∞ which can be directly calculated from activity coefficients at infinite dilution for different separation processes. Untill now [BMIM][SCN] and [EMIM][SCN] showed much higher S_{ij}^∞ (i = hexane, j = benzene) values compared to other ILs due to their small anoin [SCN].

In order to expand our knowledge about the nature of ILs, the influence of the anion structure on the thermodynamic properties of the disubstituted imidazolium based ionic liquid with [FAP], [25] [TCB], [26] and bis(oxalato)borate [BOB],[27] Anions were studied in our work. Structures of investigated ILs are presented below:

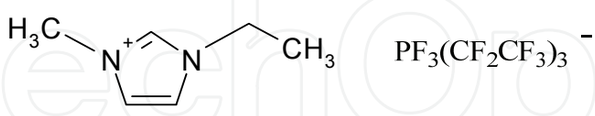

1-Ethyl-3-methylimidazolium tris(pentafluoroethyl)trifluorophosphate [EMIM][FAP]

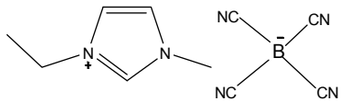

1-Ethyl-3-methylimidazolium tetracyanoborate [EMIM][TCB]

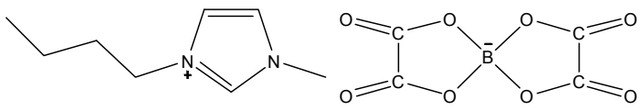

1-Butyl-3-methylimidazolium bis(oxalato)borate [BMIM][BOB]

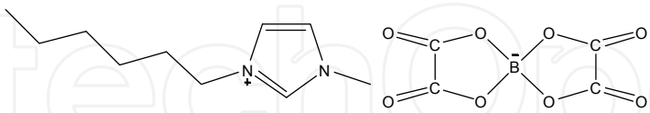

1-Hexyl-3-methyl-imidazolium bis(oxalato)borate [HMIM][BOB]

2.2 General techniques

2.2.1 Pre-processing

The purity of ILs was checked by 1H NMR, 13C NMR and 11B NMR spectroscopy. The water content was determined by Karl–Fischer titration, and were found to be less than 100 ppm. Before use, the support material and ILs were subjected to vacuum treatment with heating to remove traces of adsorbed moisture.

2.2.2 Experimental procedure

The GC column used in the experiment were constructed of stainless steel with length of 2 m and an inner diameter of 2 mm. Dichloromethane or methanol can be used as solvent to coat ILs onto the solid support 101 AW (80/100 mesh) by a rotary evaporator to ensure the homogeneous spread of the IL onto the surface of support. The solid support was weighed before and after the coating process. To avoid possible residual adsorption effects of the solutes on the solid support, the amount of ionic liquids ([EMIM][FAP], [EMIM][TCB], [BMIM][BOB] and [HMIM][BOB]) were all about 30.00 mass percent of the support material. Experiments were performed on a GC-7900 gas chromatograph apparatus, supplied by Shanghai Techcomp Limited Company in China equipped with a heated on-column injector and a flame ionization detector. The carrier gas flow rate was determined using a GL-102B Digital bubble/liquid flow meter with an uncertainty of ± 0.1 $cm^3 \cdot min^{-1}$, which was placed at the outlet of the column. The carrier gas flow rate was adjusted to obtain adequate retention times. The pressure drop (P_i-P_o) varied between (35 and 150) kPa depending on the flow rate of the carrier gas. The pressure drop was measured by a pressure transducer implemented in the GC with an uncertainty of ± 0.1 kPa. The atmospheric pressure was measured using a membrane manometer with an uncertainty of ± 0.2 kPa. Solute injection volumes ranged from 0.1 µl to 0.3 µl and were considered to be at infinite dilution on the cloumn. The injector and detector temperature were kept at 473K and 523K respectively during all experiments. The temperature of the oven was measured with a Pt100 probe and controlled to within 0.1 K. The GLC technique and equipment was tested for the system hexane in hexadecane as stationary phase at 298 K, and the results were within 2.0 % of the literature values [28].

The uncertainty of γ_i^{∞} values may be obtained from the law of propagation of errors. The following measured parameters exhibit uncertainties which must be taken into account in the error calculations with their corresponding standard deviations: the adjusted retention time t_R', ± 0.01 min; the flow rate of the carrier gas, ± 0.1 $cm^3 \bullet min^{-1}$; mass of the stationary phase, ± 0.05%; the inlet pressure, ± 0.1 KPa , outlet pressure, ± 0.2 KPa; the temperature of the oven, ± 0.1 K. The main source of uncertainty in the calculation of the net retention

volume is the determination of the mass of the stationary phase. The estimated uncertainty in determining the net retention volume V_N is about ± 2%. Taking into account that thermodynamic parameters are also subject to an error, the resulting uncertainty in the γ_i^∞ values is about ± 4%.

2.3 Theoretical basis

The equation developed by Everett [29] and Cruickshank et al [30] was used in this work to calculate the γ_i^∞ of solutes in the ionic liquid

$$\ln \gamma_{13}^{\infty} = \ln(\frac{n_3 RT}{V_N P_1^*}) - \frac{P_1^* B_{11} - V_1^*)}{RT} + \frac{P_o J(2B_{12} - V_1^{\infty})}{RT} \quad (1)$$

where V_N is the standardized retention volume of the solute, P_o is the outlet pressure, n_3 is the number of moles of the ionic liquid on the column packing, T is the column temperature, P_1^* is the saturated vapour pressure of the solute at temperature T, B_{11} is the second virial coefficient of the pure solute, V_1^* is the molar volume of the solute, V_1^∞ is the partial molar volume of the solute at infinite dilution in the solvent (assumed as the same as V_1^*) and B_{12} (where 2 refers to the carrier gas, nitrogen) is the cross second virial coefficient of the solute and the carrier gas. The values of B_{11} and B_{12} were calculated using the McGlashan and Potter equation [31]

$$\frac{B}{V_c} = 0.430 - 0.886\left(\frac{T_c}{T}\right) - 0.694\left(\frac{T_c}{T}\right)^2 - 0.0375(n-1)\left(\frac{T_c}{T}\right)^{4.5} \quad (2)$$

where n refers to the number of carbon atoms of the solute. Using the Hudson and McCoubrey combining rules, [32,33] V_{12}^c and T_{12}^c were calculated from the critical properties of the pure component.

The net retention volume V_N was calculated with the following usual relationship

$$V_N = J \bullet U_o \bullet (t_r - t_G) \bullet \frac{T_{col}}{T_f}(1 - \frac{P_{ow}}{P_o}) \quad (3)$$

where t_r is the retention time, t_G is the dead time, U_0 is the flow rate, measured by digital bubble/liquid flow meter, T_{col} is the column temperature, T_f is flowmeter temperature, P_{ow} is saturation vapor pressure of water at T_f and P_o is the pressure at the column outlet.

The factor J appearing in eqs 1 and 3 corrects for the influence of the pressure drop along the column and is given by following equation [34]

$$J = \frac{3}{2} \bullet \frac{(P_i/P_o)^2 - 1}{(P_i/P_o)^3 - 1} \quad (4)$$

where P_i and P_o are the inlet and the outlet pressure of the GC column, respectively.

The vapor pressure values were calculated using the Antoine equation and constants were taken from the literature. [35] Critical data and ionization energies used in the calculation of T_{12}^c, were obtained from literature. [35-37]

2.4 Results and discussion

The values of γ_i^∞ of different solutes (alkanes, cycloalkanes, 1-alkenes, 1-alkynes, benzene, alkylbenzenes, and alcohols) in the ionic liquids [EMIM][FAP], [EMIM][TCB], [BMIM][BOB] and [HMIM][BOB] obtained at several temperatures were listed in table 1-4.

The activity coefficients of the linear alkanes, 1-alkenes, 1-alkynes, alkylbenzenes, and alkanols increase with increasing chain length. This is also a typical behaviour for other measured ionic liquids based on methylimidazolium cation. High values of γ_i^∞ signify very small interactions between solute and solvent. The values of γ_i^∞ for alkenes and cycloalkanes are similar for the same carbon number. The cyclic structure of cycloalkanes reduces the value of γ_i^∞ in comparison to the corresponding linear alkane. The values of γ_i^∞ for alkenes are lower than those for alkanes for the same carbon number. This is caused by interaction of double bonding in alkenes with the polar ionic liquid. Alkynes, aromatic hydrocarbons and alkanols have smaller values of γ_i^∞ than alkanes, cycloalkanes, and alkenes which are revealed by stronger interactions between solvent and solute. This is the result of interactions between the triple bond in alkynes, six π-delocalized electrons in aromatics and polar group in alkanols with the polar cation and anion of the ionic liquid. For alkanes, 1-alkenes, 1-alkynes and alkanols values of γ_i^∞ decrease with increasing temperature. For the rest of the investigated solutes, benzene and alkylbenzenes values of γ_i^∞ change a little with increasing temperature.

By comparing Table 3 and 4, we can see that lengthening the alkane chain on the imidazolium (for the ILs with the [BOB] anion) causes a decrease in γ_i^∞ of the same solute (e.g. heptane, octane, benzene, 1-hexene) in the IL at the same temperature. This means that the imidazolum-based ILs with long alkyl chain reveals stronger interactions with solutes. This is also a typical behaviour for other measured ionic liquids based on methylimidazolium cations. Table 5 lists the γ_i^∞ for some solutes in 1-hexyl-3-methylimidazolium bis(trifluoromethanesulfonato)amide [HMIM][NTf_2],[10] 1-butyl-3-methylimidazolium bis(trifluoromethanesulfonato)amide [BMIM][NTf_2],[38] 1-hexyl-3-methylimidazolium thiocyanate [HMIM][SCN],[39] 1-butyl-3-methylimidazolium thiocyanate [BMIM][SCN],[20] 1-ethyl-3-methylimidazolium thiocyanate [EMIM][SCN],[21] 1-octyl-3-methylimidazolium tetrafluoroborate [OMIM][BF_4],[7] 1-butyl-3-methylimidazolium tetrafluoroborate [BMIM][BF_4],[40] 1-ethyl-3-methylimidazolium tetrafluoroborate [EMIM][BF_4],[4] 1-hexyl-3-methylimidazolium trifluoromethanesulfonate [HMIM][CF_3SO_3],[17] and 1-butyl-3-methylimidazolium trifluoromethanesulfonate [BMIM][CF_3SO_3] [19,41] at T= 298.15 K.

These data listed in Table 5 demonstrate a significant influence of the alkyl chain of ionic liquids based on methylimidazolium cation on the γ_i^∞ values. From table 5 we can also see that the activity coefficients and intermolecular interactions of different solutes in ILs are very much dependent on the chemical structure of the cation and anion.

The selectivity at infinite dilution for the ionic liquid which indicated suitability of a solvent for separating mixtures of components *i* and *j* by extraction was given by [28]

$$S_{ij}^\infty = \frac{r_{i3}^\infty}{r_{j3}^\infty} \tag{6}$$

Table 5 also summarizes the selectivities for the separation of hexane/benzene, cyclohexane/benzene, and hexane/hexene mixtures at T=298.15 K, which were calculated from the γ_i^∞ values for the ILs under study and collected from literature. As presented in table 5, the trend in S_{ij}^∞ values depends on the number of carbon atoms in the alkyl groups attached to the cation, most of the ILs with shorter alkyl chain have higher S_{ij}^∞ values while those with longer alkyl chain have smaller S_{ij}^∞ values, e.g., [OMIM][BF_4], 9 carbon atoms , S_{ij}^∞ (i = hexane, j = benzene) =10.4 , S_{ij}^∞ (i = cyclohexane, j = benzene) = 6.8; [BMIM][BF_4] , 5 carbon atoms, S_{ij}^∞ (i = hexane, j = benzene) = 37.3, S_{ij}^∞ (i = cyclohexane, j = benzene) = 19.7;

[EMIM][BF_4], 3 carbon atoms, S_{ij}^{∞} (i = hexane, j = benzene) = 49.5, S_{ij}^{∞} (i = cyclohexane, j = benzene) = 38.9. An anion with smaller carbon atoms (or no carbon atoms) tends to have a higher selectivity value, e.g., [BMIM][SCN] , [HMIM][SCN] and [EMIM][SCN] because of the small anion [SCN], all of them have much higher S_{ij}^{∞} (i = hexane, j = benzene) values than the other ILs listed in Table 5. The above trends indicate that the size of the alkyl chain on both the cation and anion plays a important role in selectivity values.

2.5 Conclusions

Activity coefficients at infinite dilution for various solutes (alkanes, cycloalkanes, 1-alkenes, 1-alkynes, benzene, alkylbenzenes, and alcohols) in the ionic liquids [EMIM][FAP], [EMIM][TCB], [BMIM][BOB] and [HMIM][BOB] were measured at different temperatures

Solute(i)	313 K	323 K	333 K	343 K	353 K	364 K
Pentane	4.44(313.1)	3.59(322.9)	2.87(333.6)	2.36(343.5)	2.01(353.5)	
Hexane	10.14(313.1)	8.15(322.9)	6.47(333.6)	5.24(343.5)	4.38(353.5)	
Heptane	19.72(313.1)	16.27(322.9)	13.00(333.6)	10.61(343.5)	8.75(353.5)	
Octane	33.30(313.1)	28.33(322.9)	23.35(333.6)	19.47(343.5)	16.14(353.5)	
Nonane	49.35(313.1)	42.85(322.9)	36.04(333.6)	31.80(343.5)	27.02(353.5)	
Cyclohexane	9.47(313.1)	7.98(322.9)	6.58(333.6)	5.52(343.5)	4.71(353.5)	
Methyl cyclohexane	13.71(313.1)	11.75(322.9)	9.91(333.6)	8.40(343.5)	7.21(353.5)	
1-Hexene	6.66(312.8)	5.49(323.6)	4.64(333.5)	3.93(343.6)	3.34(353.6)	
1-Octene	18.84(312.8)	16.39(323.6)	14.76(333.5)	12.89(343.6)	11.11(353.6)	
1-Decene	37.62(312.8)	34.74(323.6)	32.40(333.5)	29.46(343.6)	26.71(353.6)	
1-Pentyne	2.46(313.6)	2.26(322.7)	1.99(333.5)	1.82(343.4)	1.67(353.3)	
1-Hexyne	4.18(313.6)	3.87(322.7)	3.52(333.5)	3.26(343.4)	2.94(353.3)	
1-Heptyne	6.46(313.6)	6.11(322.7)	5.67(333.5)	5.29(343.4)	4.82(353.3)	
1-Octyne	9.53(313.6)	9.12(322.7)	8.65(333.5)	8.08(343.4)	7.52(353.3)	
Benzene[b]	1.06(313.1)	1.09(322.9)	1.15(333.1)	1.11(343.5)	1.10(353.3)	1.09(363.9)
Toluene[b]	1.54(313.1)	1.59(322.9)	1.69(333.1)	1.66(343.5)	1.66(353.3)	1.66(363.9)
Ethylbenzene[b]	2.40(313.1)	2.48(322.9)	2.63(333.1)	2.55(343.5)	2.54(353.3)	2.51(363.9)
o-Xylene[b]	2.14(313.1)	2.20(322.9)	2.35(333.1)	2.30(343.5)	2.30(353.3)	2.29(363.9)
m-Xylene[b]	2.29(313.1)	2.37(322.9)	2.53(333.1)	2.47(343.5)	2.47(353.3)	2.46(363.9)
p-Xylene[b]	2.37(313.1)	2.44(322.9)	2.60(333.1)	2.55(343.5)	2.54(353.3)	2.53(363.9)
Methanol	2.65(313.6)	2.29(322.7)	2.02(333.5)	1.73(343.4)	1.51(353.3)	
Ethanol	3.29(313.6)	2.86(322.7)	2.44(333.5)	2.17(343.4)	1.88(353.3)	
1-Propanol	4.46(313.6)	3.87(322.7)	3.35(333.5)	2.92(343.4)	2.59(353.3)	

[a] Measured experimental temperatures are given in parentheses. [b] Values are measured in the temperature interval 313 to 364 K.

Table 1. Experimental activity coefficients at infinite dilution, γ_i^{∞} for various solutes in the ionic liquid 1-Ethyl-3-methylimidazolium tris(pentafluoroethyl)trifluorophosphate at temperatures 313 to 364 K[a]

using GLC method. This result shows the influence of the cation's alkyl chain length on the γ_i^{∞} and S_{ij}^{∞} values. For the separation of aliphatic hydrocarbons from aromatic hydrocarbons, the ionic liquids tested in our work show moderate value of selectivity. The results summarized in Table 5 demonstrate a significant influence of the structure of anion and cation in the ionic liquids on the γ_i^{∞} values and selectivity.

Solute(*i*)	303 K	313 K	323 K	333 K	343 K
Pentane	10.26 (302.8)	8.21 (313.4)	7.05 (323.1)	5.92 (332.8)	4.88 (343.4)
Hexane	20.97 (302.8)	17.40 (313.4)	15.07 (323.1)	12.51 (332.8)	10.29 (343.4)
Heptane	37.62 (302.8)	32.19 (313.4)	28.13 (323.1)	23.82 (332.8)	19.85 (343.4)
Octane	58.88 (302.8)	52.45 (313.4)	46.72 (323.1)	40.73 (332.8)	34.94 (343.4)
Nonane	85.01 (302.8)	78.07 (313.4)	70.83 (323.1)	63.53 (332.8)	55.31 (343.4)
Cyclohexane	13.82 (302.8)	12.44 (313.4)	11.20 (323.1)	9.85 (332.8)	8.64 (343.4)
Methyl cyclohexane	20.72 (302.8)	18.86 (313.4)	16.94 (323.1)	15.15 (332.8)	13.29 (343.4)
1-Hexene	11.28 (303.5)	9.74 (313.2)	8.39 (323.3)	7.35 (333.1)	6.27 (343.1)
1-Octene	30.05 (303.5)	26.84 (313.2)	24.00 (323.3)	21.53 (333.1)	18.97 (343.1)
1-Decene	60.51 (303.5)	55.95 (313.2)	51.53 (323.3)	47.75 (333.1)	43.43 (343.1)
1-Pentyne	2.72 (303.5)	2.61 (313.3)	2.50 (323.3)	2.38 (333.1)	2.29 (343.1)
1-Hexyne	4.18 (303.5)	4.04 (313.3)	3.92 (323.3)	3.77 (333.1)	3.58 (343.1)
1-Heptyne	6.33 (303.5)	6.15 (313.3)	5.97 (323.3)	5.78 (333.1)	5.59 (342.8)
1-Octyne	9.64 (303.5)	9.42 (313.3)	9.11 (323.3)	8.84 (333.1)	8.58 (342.8)
Benzene	1.31 (303.6)	1.31 (313.3)	1.34 (323.2)	1.31 (333.3)	1.30 (343.2)
Toluene	1.90 (303.6)	1.92 (313.2)	1.98 (323.1)	1.94 (333.2)	1.92 (343.3)
Ethylbenzene	3.00 (303.6)	3.00 (313.2)	3.05 (323.1)	2.97 (333.2)	2.92 (343.3)
o-Xylene	2.49 (303.6)	2.53 (313.3)	2.58 (323.2)	2.56 (333.2)	2.54 (343.1)
m-Xylene	2.92 (303.6)	2.99 (313.2)	3.03 (323.2)	3.01 (333.1)	2.99 (343.1)
p-Xylene	2.78 (303.7)	2.85 (313.2)	2.87 (323.2)	2.85 (333.3)	2.84 (343.2)
Methanol	1.13 (303.5)	1.05 (313.3)	0.97 (323.3)	0.91 (333.1)	0.85 (343.1)
Ethanol	1.64 (303.5)	1.50 (313.3)	1.37 (323.3)	1.27 (333.1)	1.16 (343.1)
1-Propanol	2.12 (303.5)	1.92 (313.3)	1.74 (323.3)	1.60 (333.1)	1.46 (343.1)

[a] Measured experimental temperatures are given in parentheses.

Table 2. Experimental activity coefficients at infinite dilution γ_i^{∞} for various solutes in the ionic liquid [EMIM][TCB] at different temperatures[a].

Solute(*i*)	308 K	318 K	328 K	338 K	348 K
Pentane	9.11(307.8)	6.63(317.6)	5.12(328.2)	4.02(338.5)	3.23(347.7)
Hexane	27.60 (307.8)	19.18(317.7)	12.98(328.3)	9.61(338.5)	7.55(347.7)
Heptane	57.79 (307.9)	41.52 (317.6)	30.05 (328.3)	21.99 (338.5)	17.08 (347.7)
Octane	116.45(307.9)	85.74 (317.6)	62.78(328.2)	45.70(338.5)	35.48(347.7)
Nonane	194.07(307.9)	151.69 (317.6)	116.00(328.3)	87.18(338.5)	67.62(347.7)
Cyclohexane	25.44(307.8)	18.52(317.8)	13.93(328.3)	10.63(338.6)	8.52(347.6)
Methyl cyclohexane	42.37 (307.9)	31.05(317.7)	23.24(328.3)	17.76(338.6)	14.05(347.6)
1-Hexene	17.21(307.6)	12.74(317.6)	9.42(327.8)	7.80(337.7)	6.03(347.8)
1-Octene	65.85(307.6)	50.10(317.7)	39.00(327.8)	32.23(337.7)	24.95(347.8)
1-Decene	144.01(307.6)	119.05(317.7)	100.48(327.7)	87.99(337.8)	72.49(347.9)
1-Pentyne	5.49(307.8)	4.36(317.5)	3.55(327.6)	2.96(337.7)	2.47(347.8)
1-Hexyne	9.30(307.8)	7.73(317.5)	6.38(327.6)	5.43(337.7)	4.71(347.7)
1-Heptyne	14.34(307.8)	12.29(317.5)	10.52(327.7)	9.17(337.7)	7.96(347.8)
1-Octyne	21.35(307.8)	18.74(317.5)	16.31(327.7)	14.49(337.7)	12.71(347.8)
Benzene	3.29 (307.8)	3.06(317.5)	2.70(328.2)	2.48(338.5)	2.29(348.5)
Toluene	5.31(307.8)	4.71(317.5)	4.36(328.2)	3.93(338.5)	3.68(348.5)
Ethylbenzene	8.40(307.7)	7.49(317.5)	6.89(328.2)	6.22(338.4)	5.85(348.5)
o-Xylene	7.08(307.8)	6.43(317.5)	5.94(328.3)	5.50(338.4)	5.09(348.5)
m-Xylene	8.35(307.8)	7.56(317.6)	6.96(328.4)	6.33(338.4)	5.91(348.4)
p-Xylene	8.40(307.8)	7.48(317.6)	6.81(328.4)	6.33(338.4)	5.86(348.4)
Methanol	1.94(307.7)	1.73(317.5)	1.51(327.5)	1.34(337.7)	1.18(347.8)
Ethanol	3.40(307.7)	2.90(317.5)	2.48(327.6)	2.14(337.7)	1.83(347.8)
1-Propanol	4.75(307.8)	4.03(317.5)	3.40(327.6)	2.93(337.7)	2.50(347.8)

[a] Measured experimental temperatures are given in parentheses.

Table 3. Experimental activity coefficients at infinite dilution γ_i^{∞} for various solutes in the ionic liquid [BMIM][BOB] at different temperatures[a].

Solute(*i*)	308 K	318 K	328 K	338 K	348 K
Pentane	8.31(308.0)	6.89(318.2)	5.46(328.2)	4.52(338.4)	3.88(348.4)
Hexane	19.10(308.3)	15.72(318.1)	12.35(328.2)	10.18(338.3)	8.58(348.4)
Heptane	36.20(308.6)	30.89(318.2)	24.46(328.3)	20.42(338.5)	17.39(348.5)
Octane	59.37(308.5)	51.87(318.1)	43.48(328.2)	37.22(338.4)	31.84(348.6)
Nonane	89.28(308.3)	79.96(318.1)	69.05(328.2)	60.60(338.4)	53.04(348.4)
Cyclohexane	15.64(308.4)	13.18(318.1)	11.28(328.2)	9.52(338.5)	8.41(348.5)
Methyl cyclohexane	23.46(308.4)	19.90(318.1)	17.12(328.3)	15.07(338.3)	13.03(348.5)
1-Hexene	11.35(308.3)	8.97(318.2)	7.21(328.3)	5.91(338.3)	4.91(348.6)
1-Octene	30.22(308.3)	25.63(318.2)	21.88(328.3)	18.70(338.3)	16.01(348.4)
1-Decene	57.09(308.3)	51.64(318.1)	46.15(328.2)	40.86(338.4)	37.03 (348.3)
1-Pentyne	5.17(308.4)	4.67(318.3)	4.14(328.2)	3.73(338.3)	3.28(348.3)
1-Hexyne	7.87(308.4)	7.27(318.3)	6.61(328.3)	6.10(338.3)	5.52(348.3)
1-Heptyne	11.49(308.4)	10.86(318.3)	10.13(328.2)	9.41(338.4)	8.96(348.3)
1-Octyne	16.18(308.6)	15.41(318.3)	14.58(328.3)	13.75(338.5)	13.01(348.3)
Benzene	2.20(308.0)	1.98(318.2)	1.87(328.4)	1.73(338.5)	1.63(348.5)
Toluene	3.15(308.1)	2.99(318.1)	2.79(328.4)	2.65(338.5)	2.48(348.5)
Ethylbenzene	4.75(308.2)	4.42(318.2)	4.18(328.4)	3.90(338.5)	3.65(348.5)
o-Xylene	4.14(308.3)	3.91(318.3)	3.71(328.4)	3.49(338.4)	3.27(348.6)
m-Xylene	4.69(308.4)	4.44(318.3)	4.17(328.5)	3.95(338.4)	3.69(348.6)
p-Xylene	4.71(308.4)	4.43(318.3)	4.23(328.5)	3.95(338.4)	3.71(348.6)
Methanol	1.59(308.3)	1.43(318.1)	1.26(328.5)	1.14(337.5)	1.01(347.6)
Ethanol	2.43(308.3)	2.15(318.1)	1.85(328.5)	1.64(337.5)	1.41(347.7)
1-Propanol	3.08(308.3)	2.70(318.1)	2.27(328.5)	1.99(337.5)	1.70(347.7)

[a] Measured experimental temperatures are given in parentheses.

Table 4. Experimental activity coefficients at infinite dilution γ_i^{∞} for various solutes in the ionic liquid [HMIM][BOB] at different temperatures[a].

Ionic liquids	γ_i^∞ (298.15 K)				Selectivity S_{ij}^∞ values		
	Hexane	Cyclohexane	1-Hexene	Benzene	(a)	(b)	(c)
[HMIM][BOB]	24.42[a]	18.78 [a]	14.40 [a]	2.37 [a]	10.3 [b]	7.9 [b]	1.7 [b]
[BMIM][BOB]	39.39[a]	34.30 [a]	23.01 [a]	3.67 [a]	10.7[b]	9.3 [b]	1.7 [b]
[HMIM][NTf_2] [c]	8.2[a] (298K)	5.8 [a](298K)	4.6 [a](298K)	0.78 [a] (298K)	10.5 [b] (298K)	7.4 [b](298K)	1.8 [b] (298K)
[BMIM][NTf_2] [d]	15.4[a] (298K)	9.32 [a] (298K)	7.67 [a](298K)	0.88 [a] (298K)	17.5 [b] (298K)	10.6 [b] (298K)	2.0 [b] (298K)
[HMIM][SCN] [e]	/	28.2	28.7	1.91	/	14.8	/
[BMIM][SCN] [f]	226	62.3	61.6	2.13	106.1	29.3	3.7
[EMIM][SCN] [g]	327	113.9	104.5	3.43	95.4	33.2	3.1
[OMIM][BF_4] [h]	12.4[a] (298K)	8.06 [a] (298K)	7.06 [a](298K)	1.19 [a] (298K)	10.4 [b] (298K)	6.8 [b](298K)	1.8 [b](298K)
[BMIM][BF_4] [i]	64.1[a]	33.9 [a]	/	1.72 [a]	37.3 [b]	19.7 [b]	/
[EMIM][BF_4] [j]	106.9[a]	84.03[a]	/	2.16 [a]	49.5 [b]	38.9 [b]	/
[HMIM][CF_3SO_3] [k]	21.45[a]	11.04 [a]	/	1.412 [a]	15.2 [b]	7.8 [b]	/
[BMIM][CF_3SO_3] [l]	39.2[a]	23.1 [a]	/	1.8 [a]	21.8 [b]	12.8 [b]	/
[BMIM][CF_3SO_3] [m]	41.6	20.6	17.6	1.55	26.8	13.3	2.4

[a] Extrapolated values, [b] Calculated from the extrapolated values, [c] Ref.[10,], [d] Ref.[38],[e] Ref.[39], [f] Ref.[20], [g] Ref.[21],[h] Ref.[7],[i] Ref.[40], [j] Ref.[4],[k] Ref.[17],[l] Ref.[19],[m] Ref.[41].

Table 5. Values of γ_i^∞ at T = 298K and selectivity values S_{ij}^∞ at infinite dilution for different separation problems: (a) hexane/ benzene, b) cyclohexane/ benzene, (c) hexane/1-hexene.

2.6 References

[1] Visser, A. E.; Rogers, R. D. Room-Temperature Ionic Liquids: New Solvents for *f*-element Separations and Associated Solution Chemistry. *J. Solid State Chem.* 2003, *171*, 109–113.

[2] Dohnal, V.; Horakova, I. A New Variant of the Rayleigh Distillation Method for the Determination of Limiting Activity Coefficients. *Fluid Phase Equilib.* 1991, *68*, 73-185.

[3] Letcher, T. M.; Jerman, P. Activity Coefficients of Cyclohexane +*n*-Alkane Mixtures. *J. Chem. Thermodyn.* 1976, *8*, 127-131.

[4] Ge, M.-L.; Wang, L.-S.; Wu, J.-S.; Zhou, Q. Activity Coefficients at Infinite Dilution of Organic Solutes in 1-Ethyl-3-methylimidazolium Tetrafluoroborate Using Gas-Liquid Chromatography. *J. Chem. Eng. Data* 2008, *53*, 1970–1974.

[5] Mutelet, F.; Jaubert, J.-N. Measurement of Activity Coefficients at Infinite Dilution in 1-Hexadecyl-3-methylimidazolium Tetrafluoroborate Ionic Liquid. *J. Chem. Thermodyn.* 2007, *39*, 1144-1150.

[6] Zhou, Q.; Wang, L.-S.; Wu, J.-S.; Li, M.-Y. Activity Coefficients at Infinite Dilution of Polar Solutes in 1-Butyl-3-methylimidazolium Tetrafluoroborate Using Gas-Liquid Chromatography. *J. Chem. Eng. Data* 2007, *52*, 131–134.

[7] Heintz, A.; Verevkin, S. P. Thermodynamic Properties of Mixtures Containing Ionic Liquids. 6. Activity Coefficients at Infinite Dilution of Hydrocarbons, Alcohols, Esters, and Aldehydes in 1-Methyl-3-octyl-imidazolium Tetrafluoroborate Using Gas-Liquid Chromatography. *J. Chem. Eng. Data* 2005, *50*, 1515–1519.

[8] Letcher, T. M.; Soko, B.; Reddy, P. Determination of Activity Coefficients at Infinite Dilution of Solutes in the Ionic Liquid 1-Hexyl-3-methylimidazolium

Tetrafluoroborate Using Gas-Liquid Chromatography at the Temperatures 298.15 K and 323.15 K. *J. Chem. Eng .Data* 2003, *48*, 1587-1590.

[9] Letcher, T. M.; Soko, B.; Ramjugernath, D. Activity Coefficients at Infinite Dilution of Organic Solutes in 1-Hexyl-3-methylimidazolium Hexafluorophosphate from Gas-Liquid Chromatography. *J. Chem. Eng. Data* 2003, *48*, 708-711.

[10] Heintz, A.; Verevkin, S. P. Thermodynamic Properties of Mixtures Containing Ionic Liquids. 8. Activity Coefficients at Infinite Dilution of Hydrocarbons, Alcohols, Esters, and Aldehydes in 1-Hexyl-3-Methylimidazolium Bis(trifluoromethylsulfonyl)-Imide Using Gas–Liquid Chromatography. *J. Chem. Eng. Data* 2006, *51*, 434–437.

[11] Deenadayalu, N.; Letcher, T. M.; Reddy, P. Determination of Activity Coefficients at Infinite Dilution of Polar and Nonpolar Solutes in the Ionic Liquid 1-Ethyl-3-methylimidazolium Bis(trifluoromethylsulfonyl)Imidate Using Gas-Liquid Chromatography at the Temperature 303.15 or 318.15 K. *J. Chem. Eng. Data* 2005, *50*, 105–108.

[12] Letcher, T. M.; Marciniak, A.; Marciniak, M.; Domanska, U. Activity Coefficients at Infinite Dilution Measurements for Organic Solutes in the Ionic Liquid 1-Hexyl-3-methyl-imidazolium Bis(trifluoromethylsulfonyl)-Imide Using G.L.C. at *T*= (298.15, 313.15, and 333.15) K. *J. Chem. Thermodyn.* 2005, *37*, 1327–1331.

[13] Krummen, M.; Wasserscheid, P.; Gmehling, J. Measurement of Activity Coefficients at Infinite Dilution in Ionic Liquids Using the Dilutor Technique. *J. Chem. Eng .Data* 2002, *47*, 1411–1417.

[14] Heintz, A.; Kulikov, D. V.; Verevkin, S. P. Thermodynamic Properties of Mixtures Containing Ionic Liquids. 2. Activity Coefficients at Infinite Dilution of Hydrocarbons and Polar Solutes in 1-Methyl-3-ethyl-imidazolium Bis(trifluoromethyl-sulfonyl) Amide and in 1,2-Dimethyl-3-ethyl-imidazolium Bis(trifluoromethyl-sulfonyl) Amide Using Gas-Liquid Chromatography. *J. Chem. Eng. Data* 2002, *47*, 894–899.

[15] Mutelet, F.; Jaubert, J.-N.; Rogalski, M.; Boukherissa, M.; Dicko, A. Thermodynamic Properties of Mixtures Containing Ionic Liquids: Activity Coefficients at Infinite Dilution of Organic Compounds in 1-Propyl Boronic Acid-3-Alkylimidazolium Bromide and 1-Propenyl-3-alkylimidazolium Bromide Using Inverse Gas Chromatography. *J. Chem. Eng. Data* 2006, *51*, 1274–1279.

[16] David, W.; Letcher, T. M.; Ramjugernath, D.; Raal, J. D. Activity Coefficients of Hydrocarbon Solutes at Infinite Dilution in the Ionic Liquid, 1-Methyl-3-octyl-imidazolium Chloride from Gas-Liquid Chromatography. *J. Chem. Thermodyn.* 2003, *35*, 1335–1341.

[17] Yang, X.-J.; Wu, J.-S.; Ge, M.-L.; Wang, L.-S.; Li, M.-Y. Activity Coefficients at Infinite Dilution of Alkanes, Alkenes, and Alkyl benzenes in 1-Hexyl-3-methylimidazolium Trifluoromethanesulfonate Using Gas-Liquid Chromatography. *J. Chem. Eng. Data* 2008, *53*, 1220–1222.

[18] Ge, M.-L.; Wang, L.-S. Activity Coefficients at Infinite Dilution of Polar Solutes in 1-Butyl-3-methylimidazolium Trifluoromethanesulfonate Using Gas-Liquid Chromatography. *J. Chem. Eng. Data* 2008, *53*, 846–849.

[19] Ge, M.-L.; Wang, L.-S.; Li, M.-Y.; Wu, J.-S. Activity Coefficients at Infinite Dilution of Alkanes, Alkenes, and Alkyl Benzenes in 1-Butyl-3-methylimidazolium

Trifluoromethanesulfonate Using Gas-Liquid Chromatography. *J. Chem. Eng. Data* 2007, *52*, 2257–2260.

[20] Domanska, U.; Laskowska, M. Measurements of Activity Coefficients at Infinite Dilution of Aliphatic and Aromatic Hydrocarbons, Alcohols, Thiophene, Tetrahydrofuran, MTBE, and Water in Ionic Liquid [BMIM][SCN] using GLC. *J. Chem. Thermodyn.* 2009, *41*, 645–650.

[21] Domanska, U.; Marciniak, A. Measurements of Activity Coefficients at Infinite Dilution of Aromatic and Aliphatic Hydrocarbons, Alcohols, and Water in the new Ionic Liquid [EMIM][SCN] using GLC. *J. Chem. Thermodyn.* 2008, *40*, 860–866.

[22] Deenadayalu, N; Thango, S. H.; Letcher, T. M.; Ramjugernath, D. Measurement of Activity Coefficients at Infinite Dilution Using Polar and Non-polar Solutes in the Ionic Liquid 1-Methyl-3-octyl-imidazolium Diethyleneglycolmonomethylethersulfate at *T*= (288.15, 298.15, and 313.15) K. *J. Chem. Thermodyn.* 2006, *38*, 542–546.

[23] Kozlova, S. A.; Verevkin, S. P.; Heintz, A.; Peppel, T.; Kockerling, M. Activity Coefficients at Infinite Dilution of Hydrocarbons, Alkylbenzenes, and Alcohols in the Paramagnetic Ionic Liquid 1-Butyl-3-methyl-imidazolium Tetrachloridoferrate(III) using Gas–Liquid Chromatography. *J. Chem. Thermodyn.* 2009, *41*, 330–333.

[24] Kozlova, S. A.; Verevkin, S. P.; Heintz, A. Paramagnetic Ionic Liquid 1-Butyl-3-methylimidazolium Tetrabromidocobaltate (II): Activity Coefficients at Infinite Dilution of Organic Solutes and Crystal Structure. *J. Chem. Eng. Data* 2009, *54*, 1524–1528.

[25] Yan P.-F.; Yang M.; Liu X.-M.; Liu Q.-S.; Tan Z.-C.; Welz-Biermann, U. Activity Coefficients at Infinite Dilution of Organic Solutes in 1-Ethyl-3-methylimidazolium Tris(pentafluoroethyl)trifluorophosphate [EMIM][FAP] Using Gas-Liquid Chromatography. *J. Chem. Eng. Data* 2010,*55,* 2444-2450.

[26] Yan P.-F.; Yang M.; Liu X.-M.; Wang C.; Tan Z.-C.; Welz-Biermann, U. Activity coefficients at infinite dilution of organic solutes in the ionic liquid 1-ethyl-3-methylimidazolium tetracyanoborate [EMIM][TCB] using gas–liquid Chromatography. *J. Chem. Thermodyn.* 2010, *42*, 817–822.

[27] Yan P.-F.; Yang M.; Li C.-P.; Liu X.-M.; Tan Z.-C.; Welz-Biermann, U. Gas-liquid chromatography measurements of activity coefficients at infinite dilution of hydrocarbons and alkanols in 1-alkyl-3-methylimidazolium bis(oxalato)borate. *Fluid Phase Equilib.* 2010,298,287-292

[28] Tiegs, D.; Gmehling, J.; Medina, A.; Soares, M.; Bastos, J.; Alessi,P.; Kikic, I. *DECHEMA Chemistry Data Series IX,* Part 1,DECHEMA: Frankfurt/Main, 1986.

[29] Everett, D. H. Effects of Gas Imperfections on GLC Measurements. *Trans. Faraday Soc.* 1965, *61*, 1637–1645.

[30] Cruickshank, A. J. B.; Windsor, M. L.; Young, C. L. The Use of Gas-Liquid Chromatography to Determine Activity Coefficients and Second Virial Coefficients of Mixtures, *Proc. R. Soc.* 1966, *A295*, 259–270.

[31] McGlashan, M. L.; Potter, D. J. B, *Proc. R. Soc.* 1951, *267*, 448-456.

[32] Hudson, G. H.; McCoubrey, J. C. Intermolecular Forces between unlike Molecules. *Trans. Faraday Soc.* 1960, *56*, 761-771.

[33] Cruickshank, A. J. B.; Windsor, M. L.; Young, C. L. Prediction of Second Virial Coefficients of Mixtures from the Principle of Corresponding States. *Trans. Faraday Soc.* 1966, *62,* 2341-2347.

[34] Grant, D. W. *Gas-Liquid Chromatography*; van Nostrand Reinhold Company: London, 1971.

[35] Design Institute for Physical Properties, Sponsored by AIChE, *DIPPR Project 801– Full Version*; Design Institute for Physical Property Data/AIChE, 2005. Online version available at: <http://www.knovel.com/knovel2/Toc.jsp?BookID=1187&VerticalID=0>.

[36] Yaws, C. L. *Yaws' Handbook of Thermodynamic and Physical Properties of Chemical Compounds*, Knovel, 2003, online version available at: http://www.knovel.com/knovel2/Toc.jsp?BookID=667&VerticalID=0.

[37] Dean, J. A. *Lange's Handbook of Chemistry*, 15th Edition, McGraw-Hill, 1999, online version available at: http://www.knovel.com/knovel2/Toc.jsp?BookID=47&VerticalID=0.

[38] Heintz, A.; Casa´s, L. M.; Nesterov, I. A.; Emeyanenko, V. N.; Verevkin, S. P. Thermodynamic Properties of Mixtures Containing Ionic Liquids. 5. Activity Coefficients at Infinite Dilution of Hydrocarbons, Alcohols, Esters, and Aldehydes in 1-Methyl-3-butylimidazolium Bis(trifluoromethylsulfonyl) Imide Using Gas-Liquid Chromatography.*J. Chem. Eng. Data* 2005, *50*, 1510-1514.

[39] Domanska, U.; Marciniak, A.; Krolikowska, M.; Arasimowicz, M. Activity Coefficients at Infinite Dilution Measurements for Organic Solutes and Water in the Ionic Liquid 1-Hexyl-3-methylimidazolium Thiocyanate. *J. Chem. Eng. Data* Doi*:* 10.1021/je900890u.

[40] Zhou, Q.; Wang, L.-S. Activity Coefficients at Infinite Dilution of Alkanes, Alkenes, and Alkyl benzenes in 1-Butyl-3-methylimidazolium Tetrafluoroborate Using GassLiquid Chromatography. *J. Chem. Eng.Data* 2006, *51*, 1698–1701.

[41] Domanska, U.; Marciniak, A. Activity Coefficients at Infinite Dilution, Measurements for Organic Solutes and Water in the Ionic Liquid 1-Butyl-3-methylimidazolium Trifluoromethanesulfonate. *J. Phys.Chem. B* 2008, *112*, 11100–11105.

3. Thermdynamic properties of Alkyl Pyridinium Bromide Ionic Liquids determined by Adibatic Calorimetry and Thermal Analysis

3.1 Introduction

Ionic liquids are attracting increasing attention in many fields including organic chemistry, [1-4] electrochemistry, [2, 5, 6] catalysis, [7-9] physical chemistry and engineering [10-14] with their special physical and chemical properties, such as low vapor pressure, low inflammability, high inherent conductivities, thermal stability, liquidity over a wide temperature range, easy recycling, and being a good solvent for a wide variety of organic and inorganic chemical compounds. The physicochemical properties of an ionic liquid vary greatly depending on the molecular structure, e.g., miscibility with water and organic solvents, melting point, and viscosity. [15-17] Besides, ionic liquids are ''designable" as structural modifications in both the cation and anion permit the possibility to design task-specific applications when the ionic liquid contain a specific functionality covalently incorporated in either the cation or anion. [4] Alkyl pyridinium bromide ionic liquids, which are easy to synthesize and purify, are one of them and show good perspective in the applications of extraction and separation processes, synthetic chemistry, catalysis and materials science. [18-20]

However, most scientists focus on the synthesis and application of ionic liquids while few researchers put their efforts on the fundamental thermodynamic studies. [10, 20-23] As far as we know, the thermodynamic properties of ionic liquids, such as heat capacity $C_{p,m}$, glass transition temperature T_g, melting temperature T_m, thermal decomposition temperature T_{decomp}, enthalpy and entropy of phase transitions are important properties that reflect the structures and stabilities of compounds but rarely reported till now.

In the present study, two ionic liquids 1-ethylpyridinium bromide (EPBr, CAS NO. 1906-79-2) and 1-propylpyridinium bromide (PPBr, CAS NO. 873-71-2) were prepared and the structures were characterized by ^{1}H-NMR. The thermodynamic properties of EPBr and PPBr were studied with adiabatic calorimetry (AC) and thermogravimatric analysis (TG-DTG). The phase change behaviour and thermodynamic properties were compared and estimated in the series alkyl pyridinium bromide ionic liquids, which were very important in industry and their application application.

3.2 Experimental section

3.2.1 Materials

All reagents were of commercial origin with purities >99.5%. 1-bromopropane (AR grade, Sinopharm Chemical Regent Co., China), pyridine and 1-bromoethane (AR grade, Tianjin Damao Chemical Reagent Co., China) were distilled before use. After absorbing the water by molecular sieves, ethyl acetate (AR grade, Tianjin Kemiou Chemical Reagent Co., China) and acetonitrile (AR grade, Tianjin Fengchuan Chemical Reagent Co., China) were distilled and used in synthesis process.

3.2.2 Preparation of EPBr and PPBr ILs

Pyridine (1mol) was placed in a 500 ml round-bottomed flask and stirred, and 1-bromoethane or 1-bromopropane (1.1mol) was added dropwise into the flask at 70 °C. A slight excess of the 1-bromoethyl or 1-bromopropane was used to guarantee the consumption of pyridine. Ethyl acetate (80 ml) was added to reduce the viscosity of the mixture, which was left to stir under reflux at 70 °C for 48 h. The halide salt separated as a second phase from the ethyl acetate. Excess of ethyl acetate were removed by decantation.

The following reaction equations 1 and 2 gave the reaction scheme:

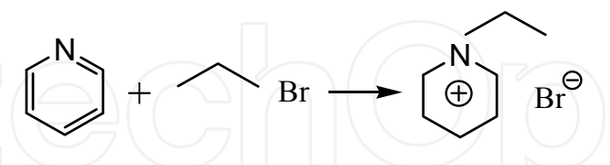

(1)

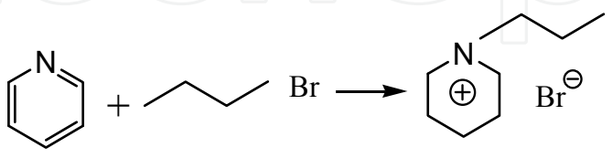

(2)

The products were recrystallized from acetonitrile. The volume of acetonitrile used for the recrystallization were approximately half of the halide salt. Acetonitrile was then decanted after crystallization, this step was repeated twice. After the third cycle, the remaining acetonitrile and 1-bromoethane or 1-bromopropane were removed under reduced pressure using rotary evaporator at 70 °C, and the bromide salts were finally dried in high vacuum at 70 °C.

3.2.3 ^{1}H-NMR of EPBr and PPBr ILs

The ^{1}H-NMR spectra were recorded on a Bruker-400Hz spectrometer and chemical shifts were reported in ppm using DMSO as an internal standard.

3.2.4 Adiabatic Calorimetry (AC).

Heat capacity measurements were carried out in a high-precision automated adiabatic calorimeter[24-26] which was established by Thermochemistry Laboratory of Dalian Institute of Chemical Physics, Chinese Academy of Sciences in PR China.The schematic diagram of the adiabatic calorimeter is shown in Figure 1.

To verify the reliability of the adiabatic calorimeter, the molar heat capacities of Standard Reference Material 720, Synthetic Sapphire (a-Al_2O_3) were measured. The deviations of our experimental results from the recommended values by NIST [27] were within ± 0.1% in the temperature range of 80-400 K.

3.2.5 Thermogravimetic Analysis (TGA)

The TG measurements of the sample were carried out by a thermogravimetric analyzer (Model: TGA/ SDTA 851e, Mettler Toledo, USA) under N_2 with a flow rate of 40 ml·min-1 at the heating rate of 10 K·min-1 from 300 to 580 K, respectively. The sample about 10-15 mg was filled into alumina crucible without pressing.

2.3 Results and discussion

2.3.1 ^{1}H-NMR of EPBr and PPBr Ils

The ^{1}H-NMR spectra δ_H （400 MHz, DMSO）of two ILs were listed in Talbe 1. Analysis of EPBr and PPBr by ^{1}H-NMR resulting in spectra is in good agreement with the literature[28] and does not show any impurities.

3.3.2 Low-temperature heat capacity

Experimental molar heat capacities of two ILs measured by the adiabatic calorimeter over the experimental temperature range are listed in Table 2 and plotted in Figure 2, respectively.

From Figure 2.a.(EPBR), a smoothed curve with no endothermic or exothermic peaks was observed from the liquid nitrogen temperature to 380 K, which indicated that the sample was thermostable in this temperature range. From 380 K to 400 K, a sharply endothermic peak corresponding to a melting process was observed with the peak temperature 391.31 K. The melting process was repeated twice and the melting temperature was determined to be 391.31 ± 0.28 K according to the two experimental results.

The values of experimental heat capacities can be fitted to the following polynomial equations with least square method: [29]

Before the fusion (8 -380 K),

$$C^0_{p,m} \ / \ \mathrm{J{\cdot}K^{-1}{\cdot}mol^{-1}} = 160.770 + 120.380x + 43.911x^2 -$$

$$- 74.730x^3 - 119.630x^4 + 78.756x^5 - 118.390x^6 \quad (3)$$

After the fusion (395 - 410 K),

$$C^0_{p,m} \ / \ \mathrm{J{\cdot}K^{-1}{\cdot}mol^{-1}} = 294.630 + 5.947x \quad (4)$$

where x is the reduced temperature; $x = [T - (T_{max} + T_{min}) / 2] / [(T_{max} - T_{min}) / 2]$; T , the experimental temperature; T_{max} and T_{min} , the upper and lower limit in the temperature region. The correlation coefficient of the fitting r^2 = 0.9981 and 0.9955 corresponding to equation 3 and 4, respectively.

However, from Figure 2.b.(BPBR), an endothermic step corresponding to a glass transition occurred with the glass transition temperature T_g = 171.595 K. A sharply endothermic peak corresponding to a melting process was observed with the peak temperature 342.83 K. The melting process was repeated twice and the melting temperature was determined to be 342.83 ± 0.69 K according to the two experimental results.

Similarly, the values of experimental heat capacities were fitted to the following polynomial equations with least square method:

Before the glass transition (78 -165 K),

$$C^0_{p,m} \ / \ \mathrm{J{\cdot}K^{-1}{\cdot}mol^{-1}} = 109.490 + 28.801x + 1.571x^2 - 9.155x^3 - 10.402x^4 + 7.121x^5 - 7.845x^6 \quad (5)$$

After glass transition and before fusion (180 -315 K),

$$C^0_{p,m} \ / \ \mathrm{J{\cdot}K^{-1}{\cdot}mol^{-1}} = 204.590 + 66.960x + 19.987x^2 + 4.091x^3 + 19.909x^4 + 27.504x^5 + 9.812x^6 \quad (6)$$

After fusion (355-400 K),

$$C^0_{p,m} \ / \ \mathrm{J{\cdot}K^{-1}{\cdot}mol^{-1}} = 310.530 + 8.712x + 3.097x^2 - 0.713x^3 - 6.183x^4 + 0.471x^5 + 3.554x^6 \quad (7)$$

The correlation coefficient of the fitting is r^2 = 0.9996, 0.9999, 0.9995 corresponding to equation 5, 6, 7, respectively.

3.3.3 Thermodynamic functions

The thermodynamic functions ($H^0_T - H^0_{298.15}$) and ($S^0_T - S^0_{298.15}$) of the two ILs relative to the reference temperature 298.15 K were calculated in the experimental temperature range with an interval of 5 K, using the polynomial equations of heat capacity and thermodynamic relationships as follows:

For EPBr,

Before melting,

$$H^0_T - H^0_{298.15} = \int_{298.15}^{T} C^0_{p,m}(s)dT \quad (8)$$

$$S^0_T - S^0_{298.15} = \int_{298.15}^{T} \frac{C^0_{p,m}(s)}{T}dT \quad (9)$$

After melting,

$$H_T^0 - H_{298.15}^0 = \int_{298.15}^{T_i} C_{p,m}^0(s)dT + \Delta_{fus}H_m^0 + \int_{T_f}^{T} C_{p,m}^0(l)dT \quad (10)$$

$$S_T^0 - S_{298.15}^0 = \int_{298.15}^{T_i} [\frac{C_{p,m}^0(s)}{T}]dT + \frac{\Delta_{fus}H_m^0}{T_m} + \int_{T_f}^{T} [\frac{C_{p,m}^0(l)}{T}]dT \quad (11)$$

where T_i is the temperature at which the solid-liquid phase transition started; T_f is the temperature at which the solid-liquid phase transition ended; $\Delta_{fus}H_m^0$ is the standard molar enthalpy of fusion; T_m is the temperature of solid-liquid phase transition.
For PPBr, the calculation of thermodynamic functions is the same with EPBr before and after the melting. Moreover, the glass transition was included in the calculation. The standard thermodynamic functions $H_T^0 - H_{298.15}^0$, $S_T^0 - S_{298.15}^0$, of the two ILs, are listed in Table 3.

3.3.4 The thermostability tested by TG-DTG

The TG-DTG curves shown in Figure 3 indicated that the mass loss of EPBr was completed in a single step. The sample keeps thermostable below 470 K. It begins to lose weight at about 480 K, reaches the maximum rate of weight loss at 541.229 K and completely loses its weight when the temperature reaches 575 K. Similar one-step decomposition process occurs for PPBr beginning at about 460 K and finishing at about 570 K while the peak temperature of decomposition is 536.021K.

3.3.5 Comparison and estimation of thermodynamic properties for alkyl pridinium bromide ionic liquids

According to experimental data in section 3.3-3.4, the thermodynamic properties as well as the structure of EPBr and PPBr were compared and estimated as follows:

a. Molar heat capacity $C_{p,m}$(EPBr) < $C_{p,m}$(PPBr) reveals that EPBr has lower lattice energy than PPBr in low temperature due to shorter carbon chain in pyridinium cation of EPBr. This rule may be applicable in the alkyl pyridium halide family and will be verified in our further research work: $C_{p,m}$(EPX) < $C_{p,m}$(PPX) < $C_{p,m}$(BPX) ; X stands for Cl, Br, I.
b. Melting temperature T_m(EPBr) > T_m(PPBr) and phase transition enthalpy $\triangle H_m$ (EPBr) >$\triangle H_m$(PPBr) are possibly because of the fact that the H-π bond effects of pyridinium cation played the major role in ionic compounds.[30] The more methylene group added in the cation, the more steric hindrance strengthened which results in decrease of the melting temperature and enthalpy.
c. Thermal decomposition temperature T_d (EPBr) > T_d (PPBr) indicates that EPBr is more thermostable than PPBr which is favorable in practical applications for EPBr .

3.4 Conclusions

Two ionic liquids 1-ethylpyridinium bromide (EPBr) and 1-propylpyridinium bromide (PPBr) were prepared and characterized. The structure and purity were verified by ^{1}H-NMR. The thermodynamic properties of EPBr and PPBr were studied with adiabatic calorimetry (AC) and thermogravimatric analysis (TG-DTG). The phase change behaviour and thermodynamic properties were compared and estimated in a series of alkyl pyridinium bromide ionic liquids. Results indicate that EPBr has higher melting and thermal decomposition temperature, phase transition enthalpy and entropy but lower heat capacity than PPBr due to the different molecular structures.

EPBr			PPBr		
Chemical shift	Hydrogen number	Radical	Chemical shift	Hydrogen number	Radical
1.529~1.566 (t)	3	CH_3	0.861~0.905 (m)	3	CH_3
/	/	/	1.906~01.997(m)	2	$-CH_2-$
4.636 ~4.69 (q)	2	$-CH_2-$	4.593 ~4.629(t)	2	$-CH_2-$
8.160~8.193 (t）	2	C(3,5)H	8.173~8.208 (t)	2	C(3,5)H
8.594~8.63(m)	1	C(4)H	8.616~8.655 (q)	1	C(4)H
9.147-9.163 (d)	2	C(2,6)H	9.144-9.158 (d)	2	C(2,6)H

Table 1. The ^1H NMR spectrum δ_H（400 MHz, DMSO）of EPBr and PPBr

T/K	$C_{p,m}$/J·K^{-1}·mol^{-1}	T/K	$C_{p,m}$/J·K^{-1}·mol^{-1}	T/K	$C_{p,m}$/J·K^{-1}·mol^{-1}
EPBr					
77.657	76.37	167.830	120.1	293.984	211.1
78.910	76.76	170.492	121.8	296.941	213.4
80.835	77.37	173.132	123.5	299.903	215.8
82.735	77.98	175.742	125.1	302.846	218.2
84.596	78.61	178.330	126.8	305.833	220.6
86.427	79.23	180.889	128.5	308.861	223.0
88.247	79.87	184.399	130.8	311.872	225.5
90.064	80.53	188.087	133.2	314.867	227.9
91.831	81.18	190.997	135.2	317.847	230.4
93.600	81.84	193.889	137.1	320.809	232.8
95.319	82.50	196.797	139.1	323.753	235.3
97.043	83.18	199.725	141.1	326.680	237.7
98.712	83.84	202.635	143.1	329.637	239.7
100.356	84.51	205.562	145.1	332.620	241.7
102.007	85.19	208.506	147.2	335.578	244.3
103.584	85.85	211.429	149.2	338.514	246.8
105.159	86.52	214.368	151.3	341.443	248.3
106.748	87.20	217.323	153.4	344.374	250.9
108.294	87.88	220.256	155.5	347.145	253.4
109.824	88.56	223.219	157.6	350.716	255.1
111.334	89.24	226.300	159.8	353.930	257.2
112.825	89.92	229.327	162.0	356.934	259.4
114.310	90.61	230.295	162.7	359.924	263.8
115.777	91.29	233.046	164.7	362.891	268.3
117.254	91.99	235.996	166.9	365.830	274.9
118.706	92.68	239.019	169.1	368.779	283.7
120.141	93.38	242.710	171.8	371.726	294.8
122.451	94.51	246.377	174.5	374.657	311.8
125.457	96.01	249.319	176.7	377.584	336.2
128.389	97.50	252.303	179.0	381.896	383.3

131.317	99.03	255.273	181.2	384.471	518.9
134.260	100.6	258.223	183.4	386.772	880.6
137.187	102.2	261.164	185.6	388.702	1385
140.095	103.8	264.144	187.9	390.114	2426
142.990	105.4	267.165	190.2	391.059	2913
145.862	107.0	270.171	192.5	393.468	368.3
148.691	108.6	273.161	194.8	397.309	290.8
151.509	110.2	276.142	197.1	400.484	292.6
154.275	111.9	279.102	199.4	403.532	295.6
157.015	113.5	282.050	201.7	406.667	298.0
159.741	115.1	285.031	204.0	409.650	300.3
162.457	116.8	288.045	206.4		
165.147	118.5	291.028	208.7		
			PPBr		
78.023	81.93	150.821	126.5	278.727	242.3
79.011	82.58	152.964	127.4	281.695	246.8
80.509	83.51	155.094	128.5	284.662	251.8
81.987	84.05	157.212	129.6	287.618	257.7
83.448	85.09	159.316	131.0	290.563	264.1
84.877	85.97	161.411	132.2	293.520	270.1
86.291	87.20	163.494	133.4	296.504	277.0
87.683	88.42	165.562	135.0	299.478	286.4
89.059	89.68	167.612	137.0	302.426	295.6
90.419	90.18	169.627	140.7	305.368	306.0
91.759	90.61	171.595	146.1	308.308	318.8
93.086	91.64	173.525	150.0	311.222	333.0
94.399	92.72	175.436	152.2	314.133	350.3
95.699	93.54	177.336	153.9	317.045	371.4
96.985	94.26	179.229	155.2	319.893	396.1
98.259	95.12	181.811	157.4	322.596	425.8
99.522	95.89	184.960	159.3	325.158	460.4
100.773	96.75	187.964	160.7	327.559	500.2
102.016	97.24	190.976	162.2	329.799	547.5
103.246	97.66	193.999	163.8	331.870	602.5
104.467	98.77	197.005	165.7	333.775	666.6
105.680	99.93	200.025	167.7	335.515	740.5
106.884	100.3	203.068	169.2	337.098	826.3
108.077	100.8	206.105	170.4	338.540	921.4
109.263	101.9	209.166	172.4	339.842	1029
110.443	102.3	212.232	174.1	341.032	1133
111.612	102.7	215.267	176.7	342.146	1156
112.773	103.7	218.270	179.2	343.563	753.9
113.931	104.5	221.226	182.0	345.633	464.8
115.078	105.1	224.186	184.1	348.293	353.8
116.220	105.4	227.228	186.9	351.393	301.7
117.354	106.1	230.236	189.0	354.574	302.4
118.482	107.0	233.079	192.1	357.586	303.4

119.602	108.0	235.879	193.9	360.598	304.5
121.367	109.6	238.705	196.9	363.600	305.8
123.762	111.6	242.272	199.5	366.595	306.9
126.132	113.2	245.916	202.6	369.613	307.8
128.476	114.7	248.905	205.8	372.656	308.6
130.800	116.1	251.877	208.6	376.372	310.4
133.098	117.4	254.857	211.8	379.412	311.2
135.379	118.5	257.855	215.2	382.441	312.5
137.636	119.5	260.823	218.3	385.470	313.9
139.877	120.7	263.802	221.6	388.488	315.1
142.099	121.8	266.790	225.1	391.504	316.3
144.303	123.0	269.785	229.3	394.600	317.4
146.491	124.2	272.790	233.3	397.710	318.5
148.663	125.5	275.759	238.0		

Table 2. Experimental molar heat capacities of EPBr and PPBr

T / K	$C_{p,m}$ / J·K^{-1}·mol^{-1}	$H_T - H_{298.15}$ / kJ·mol^{-1}	$S_T - S_{298.15}$ / J·K^{-1}mol^{-1}	$C_{p,m}$ / J·K^{-1}mol^{-1}	$H_T - H_{298.15}$ / kJ·mol^{-1}	$S_T - S_{298.15}$ / J·K^{-1}mol^{-1}
/	EPBr			PPBr		
80	78.73	-30.09	-162.1	83.06	-34.44	-183.7
85	78.71	-29.69	-157.4	86.46	-34.02	-178.6
90	79.54	-29.30	-152.9	89.79	-33.58	-173.5
95	81.03	-28.90	-148.5	92.97	-33.12	-168.6
100	83.04	-28.49	-144.2	96.03	-32.65	-163.7
105	85.40	-28.07	-140.0	99.04	-32.16	-159.0
110	88.03	-27.63	-136.0	102.1	-31.66	-154.3
115	90.81	-27.19	-132.0	105.2	-31.14	-149.7
120	93.70	-26.73	-128.1	108.5	-30.61	-145.1
125	96.62	-26.25	-124.2	111.8	-30.06	-140.6
130	99.54	-25.76	-120.4	115.1	-29.49	-136.2
135	102.4	-25.25	-116.6	118.2	-28.91	-131.8
140	105.3	-24.73	-112.9	121.1	-28.31	-127.4
145	108.1	-24.20	-109.2	123.7	-27.70	-123.1
150	110.9	-23.65	-105.5	126.0	-27.07	-118.9
155	113.6	-23.09	-101.9	128.3	-26.44	-114.7
160	116.4	-22.52	-98.22	131.1	-25.79	-110.6
165	119.1	-21.93	-94.62	135.3	-25.12	-106.5
170	121.8	-21.33	-91.03	Glass transition		
175	124.6	-20.71	-87.46	/	/	/
180	127.4	-20.08	-83.90	155.7	-23.96	-99.99
185	130.3	-19.44	-80.36	158.6	-23.18	-95.66
190	133.3	-18.78	-76.83	161.4	-22.38	-91.38
195	136.4	-18.10	-73.30	164.3	-21.56	-87.15
200	139.6	-17.41	-69.79	167.3	-20.73	-82.96

205	143.0	-16.71	-66.28	170.4	-19.89	-78.79
210	146.4	-15.98	-62.77	173.6	-19.03	-74.65
215	150.0	-15.24	-59.27	177.0	-18.15	-70.53
220	153.8	-14.48	-55.76	180.6	-17.26	-66.42
225	157.6	-13.70	-52.25	184.5	-16.35	-62.31
230	161.6	-12.91	-48.73	188.6	-15.41	-58.21
235	165.6	-12.09	-45.21	192.9	-14.46	-54.11
240	169.7	-11.25	-41.68	197.4	-13.49	-50.00
245	173.9	-10.39	-38.14	202.1	-12.49	-45.88
250	178.1	-9.511	-34.59	207.1	-11.46	-41.75
255	182.3	-8.610	-31.04	212.3	-10.42	-37.60
260	186.5	-7.688	-27.47	217.7	-9.341	-33.43
265	190.6	-6.745	-23.89	223.5	-8.238	-29.22
270	194.7	-5.781	-20.30	229.7	-7.105	-24.99
275	198.7	-4.798	-16.71	236.4	-5.940	-20.72
280	202.5	-3.795	-13.10	243.8	-4.740	-16.39
285	206.2	-2.773	-9.496	252.3	-3.500	-12.00
290	209.8	-1.733	-5.886	262.2	-2.215	-7.532
295	213.3	-0.675	-2.275	273.9	-0.876	-2.953
298.15	215.3	0.000	0.000	282.4	0.000	0.000
300	216.6	0.400	1.335	288.0	0.528	1.764
305	219.7	1.490	4.943	305.2	2.009	6.661
310	222.9	2.597	8.545	326.5	3.587	11.79
315	225.9	3.719	12.14	352.9	5.283	17.22
320	229.1	4.856	15.73	Phase transition		
325	232.3	6.010	19.32	/	/	/
330	235.8	7.180	22.90	/	/	/
335	239.6	8.368	26.48	/	/	/
340	244.0	9.577	30.07	/	/	/
345	249.0	10.81	33.67	/	/	/
350	255.0	12.07	37.29	/	/	/
355	262.2	13.36	40.96	302.5	16.98	51.22
360	270.9	14.69	44.68	304.4	18.50	55.46
365	281.4	16.07	48.47	306.3	20.02	59.67
370	294.1	17.51	52.38	307.9	21.56	63.85
375	309.4	19.02	56.42	309.6	23.10	68.00
380	327.8	20.61	60.65	311.5	24.65	72.11
385	Phase transition			313.7	26.22	76.20
390	/	/	/	315.7	27.79	80.26
395	288.7	33.16	92.83	317.5	29.37	84.29
400	292.6	34.61	96.49	319.5	30.97	88.30
405	296.6	36.09	100.2			
410	300.6	37.58	103.8			

Table 3. Smoothed heat capacities and thermodynamic functions of EPBr and PPBr.

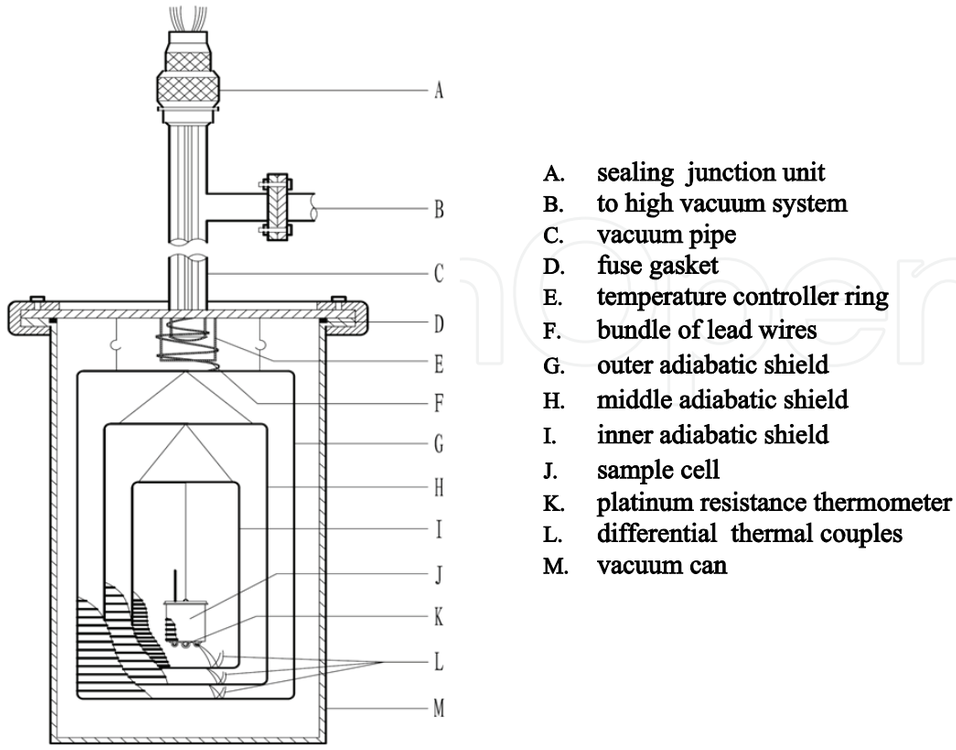

Fig. 1. A. Schematic diagram of main body of the adiabatic calorimeter

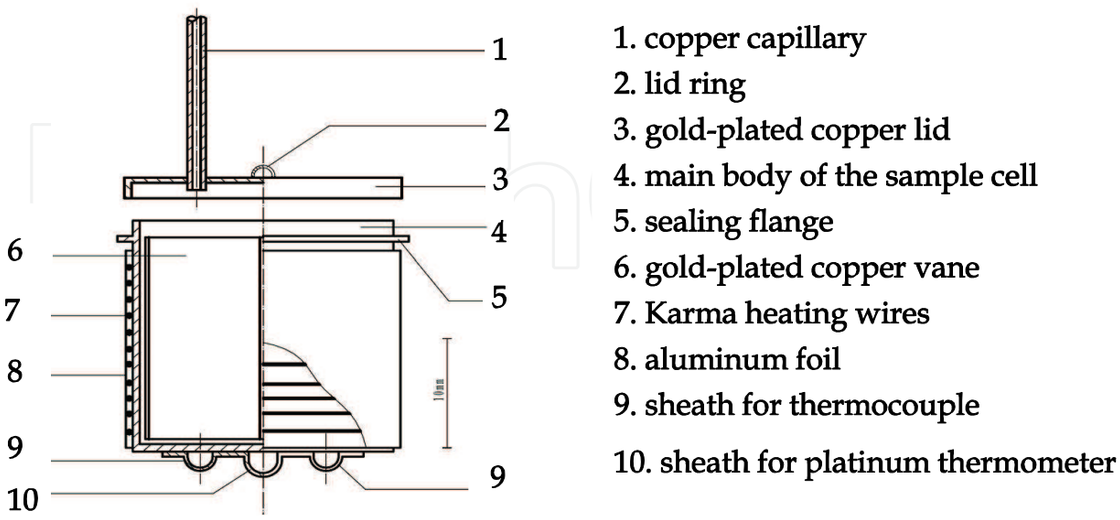

Fig. 1. B. Schematic diagram of sample cell of the adiabatic calorimeter

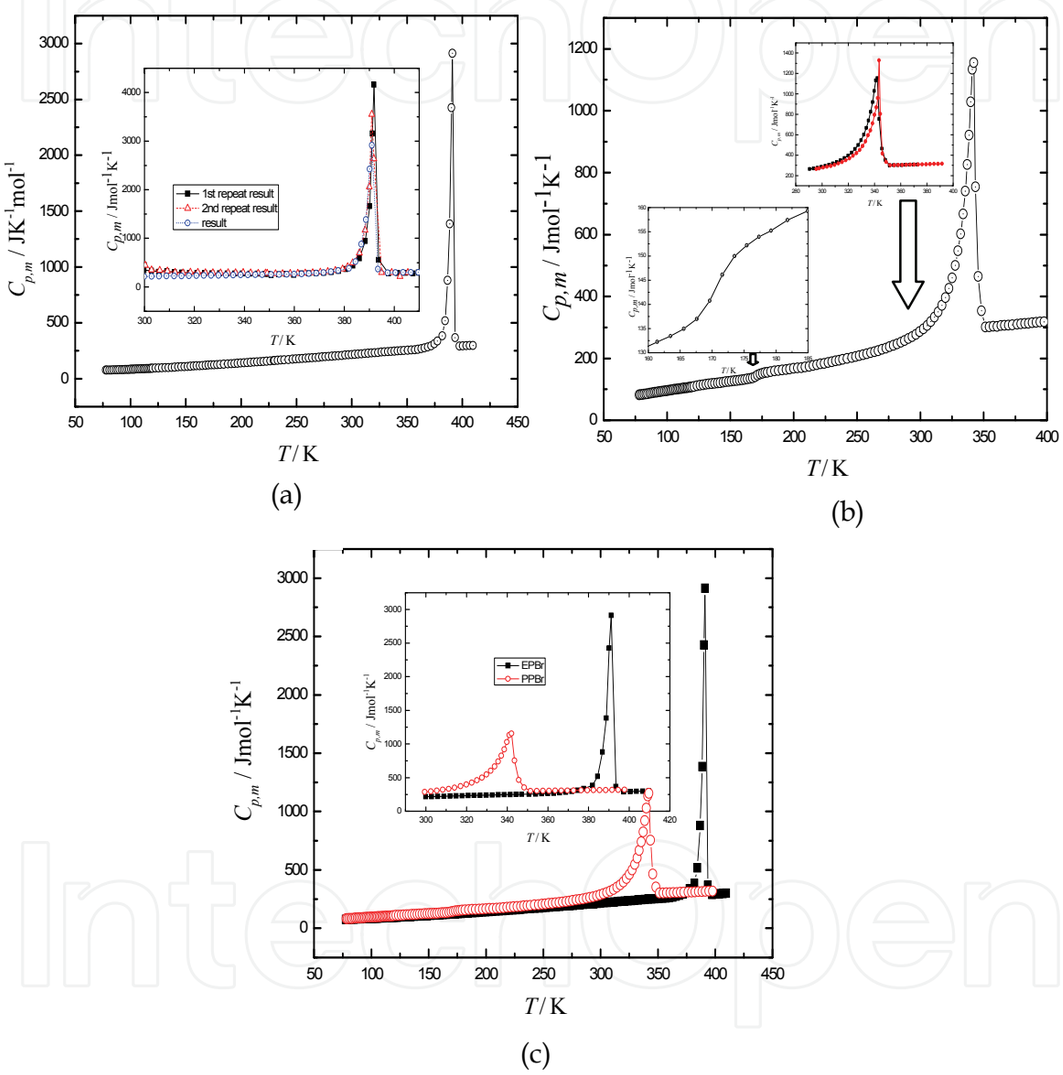

Fig. 2. Experimental molar heat capacity $C_{p,m}$ as a function of temperature (a) EPBr; (b) PPBr; (c) Comparison from 300 to 400 K

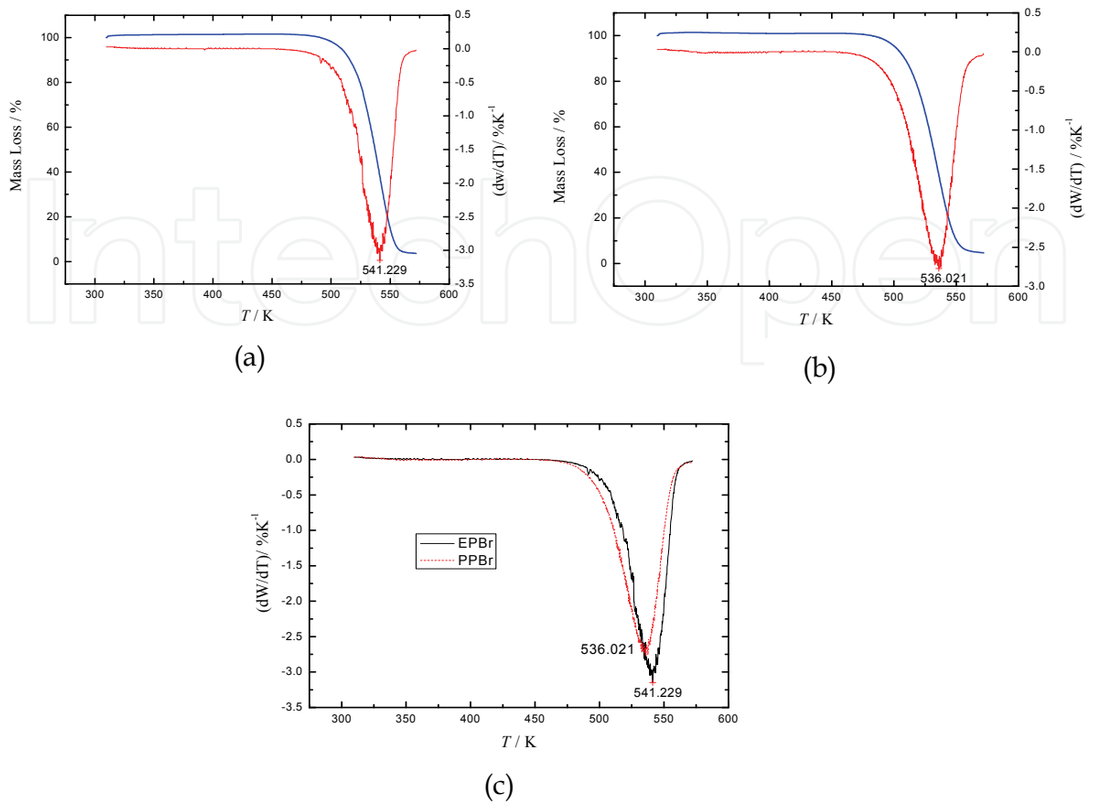

Fig. 3. TG-DTG curves under high purity nitrogen.(a) EPBr; (b) PPBr; (c) DTG curves of two ILS

3.5 References

[1] Earle M.J.; Seddon, K.R. Ionic liquids. *Pure Appl. Chem.*, 2000, *72*, 1391-1398.
[2] Rogers, R.D.; Seddon, K.R. Eds. ACS Symposium Series 818, American Chemical Society: Washington, DC, 2002.
[3] Rogers, R.D., Seddon, K.R., Eds. ACS Symposium Series 856, American Chemical Society: Washington, DC, 2003, Chapter 12.
[4] Ikegami S.; Hamamoto H. *Chem. Rev.*, 2009, 109, 583-593.
[5] Tu, W.W.; Lei, J.P.; Ju, H.X. *Chem-Eur. J.*, 2009, *15*, 779-784.
[6] Xu, H.; Xiong, H.Y.; Zeng, Q.X.; Jia, L.; Wang, Y.; Wang, S.F. *Electrochem. Commun.*, 2009, *11*, 286-289.
[7] Parvulescu, V.I.; Hardacre, C. *Chem. Rev.*, 2007, *107*, 2615-2665.
[8] Singh, M.; Singh, R.S.; Banerjee, U.C. *J. Mol. Catal. B-Enzym.*, 2009, *56*, 294-299.
[9] Karout, A.; Pierre, A.C. *Catal. Commun.*, 2009, *10*, 359-361.
[10] Verevkin, S.P.; Kozlova, S.A.; Emel'yanenko, V. N.; Goodrich, P.; Hardacre, C. *J. Phys. Chem. A*, 2008, *112*, 11273-11282.
[11] Lassegues, J.C.; Grondin,J.; Aupetit, C.; Johansson, P. *J. Phys. Chem. A*, 2009, *113* (1), 305-314.
[12] Chang, T.M.; Dang, L.X. *J. Phys. Chem. A*, 2009, *113* (10), 2127–2135.

[13] Hayamizu, K.; Tsuzuki, S. Seki, S. *J. Phys. Chem. A*, 2008, *112* (47), 12027-12036.
[14] Oxley, J.D.; Prozorov, T. Suslick, K.S. *J. Am. Chem. Soc.*, 2003, *125* (37), 11138-11139.
[15] Sobota, M.; Dohnal, V.; Vrbka, P. *J. Phys. Chem. B*, 2009, *113*, 4323-4332.
[16] Tong, J.; Liu, Q. S.; Wei, G.; Yang, J. Z. *J. Phys. Chem. B*, 2007, *111*, 3197-3200.
[17] Tong, J.; Liu, Q. S.; Wei, G. X.; Fang, D. W.; Yang, J. Z. *J. Phys. Chem. B*, 2008, *112*, 4381-4386.
[18] Lopes, J.N.C.; Padua, A.A.H. *J. Phys. Chem. B*, 2006, *110*, 19586-19592.
[19] Pham, T.P.T, Cho, C.W.; Jeon, C.O.; Chung, Y.J.; Lee, M.W.; Yun, Y.S. *Environ. Sci. Technol.*, 2009, *43*, 516-521.
[20] Jacob, M. C.; Mark, J. M.; JaNeille, K. D.; Jessica, L. A.; Joan, F. B. *J. Chem. Thermodynamics*, 2005, *37*, 559-568.
[21] Tong, J.; Liu, Q. S.; Peng, Z.; Yang, J. Z. *J. Chem. Eng. Data*, 2007, *52*, 1497-1500.
[22] Tong, J.; Liu, Q. S.; Wei, G.; Yang, J. Z. *J. Chem. Eng. Data*, 2009, *54*, 1110-1114.
[23] Del Popolo, M. G.; Mullan,C. L.; Holbrey,J. D.; Hardacre, C.; Ballone, P. *J. Am. Chem. Soc.*, 2008, *130*, 7032–7041.
[24] Tong, B.; Tan, Z.C.; Shi, Q.; Li, Y.S.; Yue, D.T.; Wang, S.X. *Thermochimi. Acta*, 2007, *457*, 20-26.
[25] Tong, B.; Tan, Z.C.; Zhang, J.N.; Wang, S.X. *J. Therm. Anal. Calorim.*, 2009, *95*, 469-475, 2009
[26] Tan, Z.C.; Shi, Q.; Liu, B.P.; Zhang, H.T. *J. Therm. Anal. Calorim.*, 2008, *92*, 367-374.
[27] Archer, D.G. *J. Phys. Chem. Ref. Data.* 1993, *22*, 1411-1453.
[28] Katritzky, A.R.; Dega-Szafran, Z. *Magn. Reson. Chem.*, 1989, *27*, 1090-1093.
[29] Tong, B.; Tan, Z.C.; Lv, X.C.; Sun, L.X.; Xu, F.; Shi, Q.; Li, Y.S. *J. Therm. Anal. Calorim.*, 2007, *90*, 217-221.
[30] Jiang, D.; Wang Y.Y.; Liu, J.; Dai. L.Y. *Chinese Chem. Lett.* 2007, *5*, 371-375.

4. Estimation and prediction of physicochemical properties of imidazolium-based ionic liquids

4.1 Introduction

The physicochemical properties of ionic liquids (ILs) at 298.15 K could be estimated and predicted in terms of empirical and semi-empirical equations, as well as the interstice model theory. In the present study, the properties of molecular volume, density, standard molar entropy, lattice energy, surface tension, parachor, molar enthalpy of vaporization, interstice volume, interstice fractions, thermal expansion coefficient were discussed. These properties first were estimated through the data of experimental density and surface tension for 1-ethyl-3-methylimidazolium ethylsulfate ([C_2mim][$EtSO_4$]), 1-butyl-3-methylimidazolium octylsulfate ([C_4mim][$OcSO_4$]) and 1-ethyl-3-methylimidazolium bis(trifluoromethanesulfonato)amide ([C_2mim][NTf_2]). The properties of molecular volume and parachor of the three homologues imidazolium-based ILs [$C_n$mim][$EtSO_4$], [$C_n$mim][$OcSO_4$] and [$C_n$mim][NTf_2] (n=1-6) were predicted, and then, the density and surface tension were obtained. Other properties were also calculated using the obtained density and surface tension values. The predicted density was compared to the experimental values for [C_4mim][NTf_2] and [C_2mim][$OcSO_4$], which shows that the deviation between experimental and predicted data are within the experimental error. Finally, we compared the values of molar enthalpy of vaporization estimated by Kabo's empirical equation with those predicted by Verevkin's simple rule for [C_2mim][$EtSO_4$],

[C_4mim][$OcSO_4$], [C_2mim][NTf_2], [C_4mim][NTf_2], *N*-butyltrimethylammonium bis(trifluoromethanesulfonato)amide [N_{4111}][NTf_2], *N*-methyltrioctylammonium bis(trifluoromethanesulfonato)amide ([N_{8881}][NTf_2]) and *N*-octyl-3-methylpyridinium tetrafluoroborate ([$m_3$opy][BF_4]), and found that the values obtained by these two equations are in good agreement with each other. Therefore, we suggest that the molar enthalpy of vaporization of ILs can be predicted by Verevkin's simple rule when experimental data for density and surface tension are not available.

ILs as organic salts, often exhibits interesting properties such as low melting points, good solvation properties and non-volatility, which are required both by industrial and scientific communities for their broad application range as electrolytes in batteries and supercapacitors[1-2], reaction media in nanoscience[3], physical chemistry[4-5] and many other areas. Therefore, the data of physicochemical properties of ILs are of fundamental for their future application and valuable for an insight into the origins of their unique behavior. Recently, more and more publications reported the experimental physicochemical properties of various ILs [6-15]. Although there is a significant amount of data related to imidazolium-based ILs, properties of homologue of [$C_n$mim][$EtSO_4$], [$C_n$mim][$OcSO_4$] and [$C_n$mim][NTf_2] (*n*=1-6) covered in this research are still limited [16-17]. Hence, we estimated various physicochemical properties of [C_2mim][$EtSO_4$], [C_4mim][$OcSO_4$], and [C_2mim][NTf_2] by using their experimental density and surface tension data. In the next step, the physicochemical properties of their homologues [$C_n$mim][$EtSO_4$], [$C_n$mim][$OcSO_4$] and [$C_n$mim][NTf_2] (*n*=1-6) were predicted from the estimated values of their molecular volume and parachor. In the present study, the ionic liquid cations are 1-alkyl-3-methylimidazolium [$C_n$mim]$^+$, tetra-alkyl ammonium [TAA]$^+$, *N*-octyl-3-methylpyridinium [$m_3$opy]$^+$; the anions of the ILs are ethylsulfate [$EtSO_4$]$^-$, octylsulfate [$OcSO_4$]$^-$, bis(trifluoromethanesulfato)amide [NTf_2]$^-$ and Tetrafluoroborate [BF_4]$^-$.

4.2 Volumetric, entropy and lattice energy

The molecular volume, V_m, can be calculated from experimental density using the following equation:

$$V_m = M/(N \cdot \rho) \tag{1}$$

where M is molar mass, ρ is density and N is Avogadro's constant.

According to Glasser's theory[18], the standard molar entropy could be estimated from the equation:

$$S^0(298.15\ \mathrm{K}) = 1246.5 V_m + 29.5 \tag{2}$$

where V_m is the molecular volume.

The lattice energy, U_{POT}, was estimated according to the following equation [18]:

$$U_{POT}(298.15\ \mathrm{K}) = 1981.2(\rho/M)^{1/3} + 103.8 \tag{3}$$

where M is molar mass and ρ is density.

The contribution methylene (-CH_2-) group to the molecular volume is 0.0272 nm^3 for [$C_n$mim][BF_4][18], 0.0282 nm^3 for [$C_n$mim][NTf_2][18], 0.0270 nm^3 for [$C_n$mim][$AlCl_4$][15] and 0.0278 nm^3 for [$C_n$mim][Ala][14]. Due to the similar values of the contribution per -CH_2- to the molecular volume, the group of methylene in the alkyl chains of the imidazolium-based ILs could be considered to have the similar chemical environment. Hense, the mean value of

the contribution can be calculated to be 0.0275 nm^3, the physicochemical properties (density, standard entropy, lattice energy) of the homologues of $[C_n mim][EtSO_4]$ and $[C_n mim][OcSO_4]$ (n=1-6) could be predicted. Using the value 0.0282 nm^3 for the contribution per -CH_2- to the molecular volume for the homologues of $[C_n mim][NTf_2]$[18] (n=1-6), the physicochemical properties of all IL homologues can be predicted. The calculated density value 1.4381 g·cm^{-3} for $[C_4mim][NTf_2]$ is in good agreement with the experimental values 1.4366[6], 1.43410 and 1.43573 g·cm^{-3}[19]. The predicted density value 1.0881 g·cm^{-3} for $[C_2mim][OcSO_4]$ is also in good agreement with the experimental value of 1.0942 g·cm^{-3} [20].

All of the estimated and predicted physicochemical property data are listed in Tables 1—3. Based on the plotting, S^{θ}, against the number of the carbons, n, in the alkyl chain of the ILs (see Fig. 1), the contribution per methylene group to the standard entropy, S^{θ}, was calculated to be 35.1 J·K^{-1}·mol^{-1} for $[C_n mim][NTf_2]$, 34.3 J·K^{-1}·mol^{-1} for $[C_n mim][EtSO_4]$ and 34.3 J·K^{-1}·mol^{-1} for $[C_n mim][OcSO_4]$. The above calculated values are in good agreement with the literature values of 35.1 J·K^{-1}·mol^{-1} for $[C_n mim][NTf_2]$[18], 33.9 J·K^{-1}·mol^{-1} for $[C_n mim][BF_4]$[18], 33.7 J·K^{-1}·mol^{-1} for $[C_n mim][AlCl_4]$[15] and 34.6 J·K^{-1}·mol^{-1} for $[C_n mim][Ala]$[14]. According to these various values for the contribution per methylene group to the standard entropy in the homologue series with different anions, it could be concluded that these contributions are relatively similar for all imidazolium-based ILs.

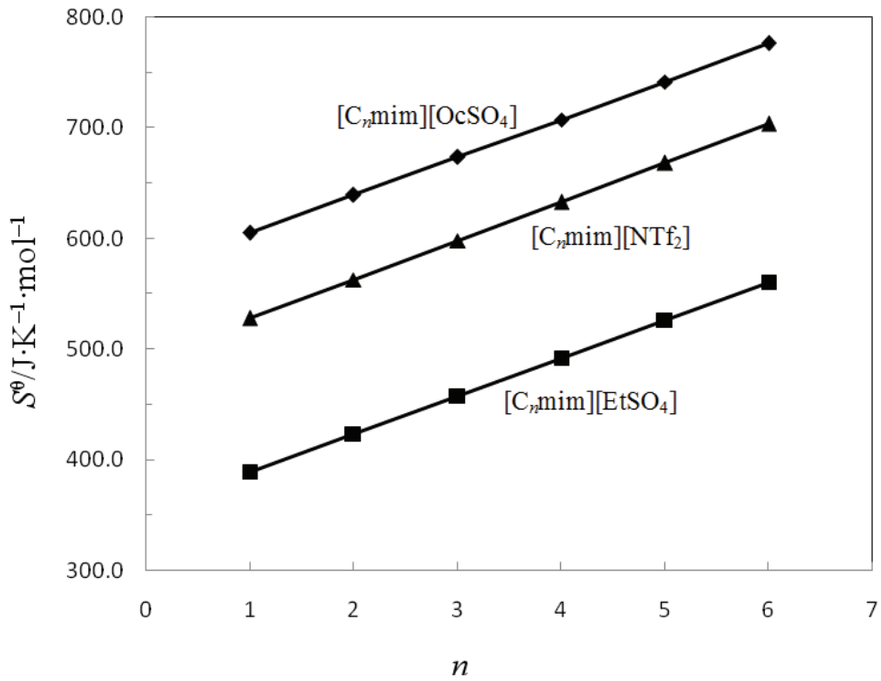

Fig. 1. Plots of S^{θ} against the number of the carbon (n), in the alkyl chain of the ILs at 298.15 K
−♦− S^{θ} =570.7+34.27n , R=0.9999 for $[C_n mim][OcSO_4]$;
−▲− S^{θ} =492.7+35.14n, R=0.9999 for $[C_n mim][NTf_2]$;
−■− S^{θ} =355.2+34.29n, R=0.9999 for $[C_n mim][EtSO_4]$

4.3 Parachors and Molar enthalpy of vaporization

The parachor, P, was estimated from the following equation [21]:

$$P=(M\gamma^{1/4})/\rho \tag{4}$$

where M is molar mass, ρ is the density and γ is the surface tension.
According to literature [15], the contribution per methylene (–CH_2–) group to parachor is 31.1. The values of parachor for the homologue series of the imidazolium-based ILs [$C_n$mim][$EtSO_4$], [$C_n$mim][$OcSO_4$] and [$C_n$mim][NTf_2] (n = 1-6) were predicted.
The values of molar enthalpy of vaporization were estimated in terms of Kabo's empirical equation [22]:

$$\Delta_l g H_m^{\theta}(298.15\ \mathrm{K})=0.01121(\gamma V^{2/3}N^{1/3})+2.4 \tag{5}$$

where V is molar volume, γ is the surface tension and N is the Avogadro's constant.
According to Eq.(4), the surface tension can be calculated from predicted density and parachor data. The calculated value 31.71 mJ · m^{-2} for the surface tension of [C_4mim][NTf_2] is in good agreement with the experimental value 32.80 mJ · m^{-2} [6]. The molar enthalpy of vaporization, $\Delta_l g H_m^{\theta}$, then can be obtained based on the predicted density and surface tension data.
All of these data are listed in Tables 1—3 and 5.
The plots of density, ρ, and surface tension, γ, against the number of carbon, n, in alkyl chain of ILs at 298.15 K are shown in Fig. 2 and 3.
From the Figs. 2 and 3, it can be seen that as for density: [$C_n$mim][NTf_2]>[$C_n$mim][$EtSO_4$]>[$C_n$mim][$OcSO_4$] and as for surface tension: [$C_n$mim][$EtSO_4$]>[$C_n$mim][NTf_2]>[$C_n$mim][$OcSO_4$].

4.4 Interstice model theory

According to the interstice model[23-24] the interstice volume, V, could be estimated by classical statistical mechanics:

$$V = 0.6791(k_b T/\gamma)^{3/2} \tag{6}$$

where k_b is the Boltzmann constant, T is the thermodynamic temperature and γ is the surface tension of ILs.
The molar volume of ionic liquids, V, consists of the inherent volume, Vi, and the volume of the interstices; whereas the molar volume of the interstice is $\sum v=2Nv$:

$$V=V_i+2Nv \tag{7}$$

If the expansion volume of IL only results from the expansion of the interstices when the temperature increase, then, the thermal expansion coefficient, α, can be predicted from the interstice model:

$$\alpha=(1/V)(\partial V/\partial T)_p=3Nv/VT \tag{8}$$

All data obtained by this estimation and prediction are listed in Tables 1—3.
The prediction and estimation values in Tables 1—3 of the thermal expansion coefficients are good agreement with experimental values. It also can be noticed that the values of interstice fractions, $\sum v/V$, differentiate only about 10—15% for all ILs studied in the present research and these values are in good agreement with the values of volume expansion resulted in the process from solid to liquid state for the majority of materials. Therefore the interstice model is applicable and the interstice model theory can be used to the thermal expansion coefficient of imidazolium-based ILs.

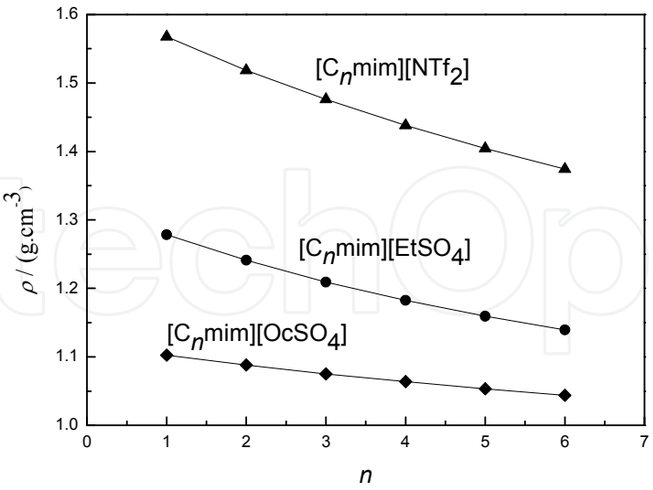

Fig. 2. Plot of density (ρ) against n (n=1–6) at 298.15 K

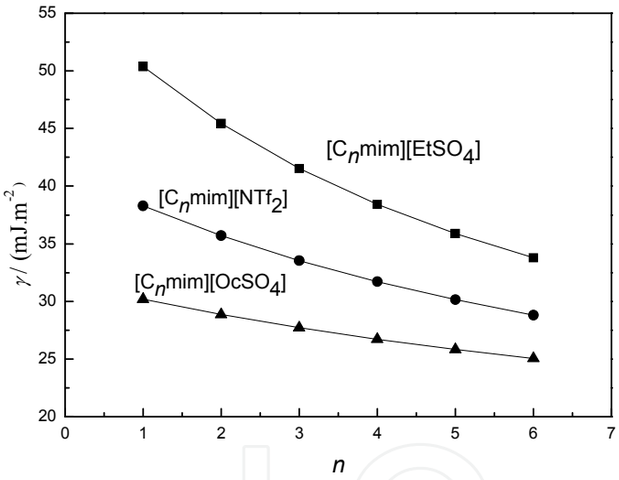

Fig. 3. Plots of surface tension (γ) against n (n=1–6) at 298.15 K

IL	V_m / nm^3	ρ / g·cm^{-3}	S^θ / J·K^{-1}·mol^{-1}	U_{POT} / kJ·mol^{-1}	V / cm^3·mol^{-1}	p
[C$_1$mim][EtSO$_4$]^b	0.2880	1.2784	389.5	459	173.9	463.2
[C$_2$mim][EtSO$_4$]^a	0.3163	1.2411[6]	423.7	448	190.4	494.3
[C$_3$mim][EtSO$_4$]^b	0.3438	1.2094	458.0	439	207.0	525.4
[C$_4$mim][EtSO$_4$]^b	0.3713	1.1826	492.3	430	223.5	556.5
[C$_5$mim][EtSO$_4$]^b	0.3988	1.1593	526.6	423	240.1	587.6
[C$_6$mim][EtSO$_4$]^b	0.4263	1.1393	560.9	416	256.6	618.7

IL	$\Delta_l g H_m^\theta$ / kJ·mol^{-1}	$10^{24}V$ / cm^3	$\sum V$ / cm^3	$10^2\sum V/V$	$10^4\alpha$ / K^{-1}	γ / mJ·m^{-2}
[C_1mim][$EtSO_4$][b]	151.0	15.86	19.10	10.98	5.53	50.38
[C_2mim][$EtSO_4$][a]	144.7	18.52	22.30	11.71	5.89,5.58[6]	45.44[6]
[C_3mim][$EtSO_4$][b]	139.9	21.19	25.52	12.33	6.20	41.53
[C_4mim][$EtSO_4$][b]	136.3	23.82	28.68	12.83	6.45	38.42
[C_5mim][$EtSO_4$][b]	133.6	26.38	31.76	13.23	6.66	35.89
[C_6mim][$EtSO_4$][b]	131.5	28.89	34.78	13.55	6.82	33.78

[a] property data for this IL were estimated values; [b] property data for this IL were predicted values

Table 1. Estimated and predicted values of physicochemical properties of [$C_n$mim][$EtSO_4$] (n=1-6) at 298.15K

IL	V_m / nm^3	ρ / g·cm^{-3}	S^θ / J·K^{-1}·mol^{-1}	U_{POT} / kJ·mol^{-1}	V / cm^3·mol^{-1}	p
[C_1mim][NTf_2][b]	0.3998	1.5676	527.9	422	240.7	598.7
[C_2mim][NTf_2][a]	0.4280	1.5187[6]	563.0	415	257.7	629.8
[C_3mim][NTf_2][b]	0.4562	1.4759	598.2	409	274.6	660.9
[C_4mim][NTf_2][b]	0.4844	1.4381	633.3	403	291.6	692.0
[C_4mim][NTf_2][a]	0.4849	1.4366[6]	633.9	402	291.9	698.6
[C_4mim][NTf_2][a]	0.4857	1.43410[19]	635.0	402	292.4	
[C_4mim][NTf_2][a]	0.4852	1.43573[19]	634.3	402	292.1	
[C_5mim][NTf_2][b]	0.5126	1.4044	668.5	397	308.6	723.1
[C_6mim][NTf_2][b]	0.5408	1.3743	703.6	392	325.6	754.2

IL	$\Delta_l g H_m^\theta$ / kJ·mol^{-1}	$10^{24}v$ / cm^3	$\sum v$ / cm^3	$10^2\sum V/V$	$10^4\alpha$ / K^{-1}	γ / mJ·m^{-2}
C_1mim][NTf_2][b]	142.6	23.94	28.82	11.98	6.02	38.29
C_2mim][NTf_2][a]	139.2	26.59	32.01	12.43	6.25,6.66[6]	35.70[6]
C_3mim][NTf_2][b]	136.5	29.20	35.16	12.80	6.44	33.54
C_4mim][NTf_2][b]	134.4	31.76	38.24	13.11	6.60	31.71
C_4mim][NTf_2][a]	139.0	30.19	36.35	12.45	6.27,6.73[6]	32.80[6]
[C_4mim][NTf_2][a]						
[C_4mim][NTf_2][a]						
C_5mim][NTf_2][b]	132.7	34.26	41.25	14.13	6.72	30.15
C_6mim][NTf_2][b]	131.4	36.70	44.18	14.32	6.83	28.80

[a] property data for this IL were estimated values; [b] property data for this IL were predicted values

Table 2. Estimated and predicted values of physicochemical properties of [$C_n$mim][NTf_2] (n=1-6) at 298.15 K

IL	V_m / nm^3	ρ / g·cm^{-3}	S^θ / J·K^{-1}·mol^{-1}	U_{pot} / kJ·mol^{-1}	V / cm^3·mol^{-1}	p
[C_1mim][$OcSO_4$]^b	0.4617	1.1025	605.0	407	277.9	651.5
[C_2mim][$OcSO_4$]^b	0.4892	1.0881	639.3	402	294.5	682.6
[C_2mim][$OcSO_4$]^a	0.4866	1.0942[20]	636.0	402	293.0	
[C_3mim][$OcSO_4$]^b	0.5167	1.0753	673.6	396	311.1	713.7
[C_4mim][$OcSO_4$]^a	0.5442	1.0638[6]	707.8	391	327.6	744.8
[C_5mim][$OcSO_4$]^b	0.5717	1.0534	742.1	387	344.2	775.9
[C_6mim][$OcSO_4$]^b	0.5992	1.0439	776.4	382	360.7	807.0

IL	$\Delta_l g H_m^\theta$ / kJ·mol^{-1}	$10^{24}V$ / cm^3	$\sum V$ / cm^3	$10^2\sum V/V$	$10^4\alpha$ / K^{-1}	γ / mJ·m^{-2}
[C_1mim][$OcSO_4$]^b	124.1	34.19	41.17	14.81	7.45	30.19
[C_2mim][$OcSO_4$]^b	123.3	36.58	44.05	14.96	7.52	28.86
[C_2mim][$OcSO_4$]^a						
[C_3mim][$OcSO_4$]^b	122.8	38.86	46.79	15.04	7.57	27.72
[C_4mim][$OcSO_4$]^a	122.6	41.09	49.47	15.10	7.59, 6.21[6]	26.71[6]
[C_5mim][$OcSO_4$]^b	122.5	43.20	52.02	15.11	7.60	25.83
[C_6mim][$OcSO_4$]^b	122.6	45.24	54.47	15.10	7.60	25.05

[a] property data for this IL were estimated values; [b] property data for this IL were predicted values

Table 3. Estimated and predicted values of the physicochemical properties of [$C_n$mim][$OcSO_4$] (n=1-6) at 298.15 K

4.5 Prediction of enthalpy of vaporization

Recently, Verevkin[25] has published an article titled "Predicting Enthalpy of Vaporization of Ionic Liquids: A Simple Rule for a Complex Property" in which he predicted molar enthalpy of vaporization of ILs by a simple rule in case of lack of experimental data. He proposed following simple rule:

$$\Delta_l g H_m^\theta(\mathrm{IL}) = \sum n_i \Delta H_i + \sum n_j \Delta H_j \quad (9)$$

where ΔH_i is the contribution of the ith element, n_i is the number of the element of the ith type in ILs, ΔH_j is the contribution of the jth structural correction and n_j is the number of the element of the jth structural correction in ILs. The parameters[25] for predicting the molar enthalpy of vaporization of ILs are listed in Table 4.

Verevkin pointed out that "a special structural correction could be also necessary for quaternary ammonium based ILs" [25]. Herein, the structure of the quaternary ammonium cation is regarded to be the ring of imidazolium cation, therefore, their structural correction parameter is ΔH=27.1 kJ·mol^{-1}. The predicted data are listed in Table 5. From this table, the values of the molar enthalpy of vaporization, $\Delta_l g H_m^\theta$, predicted by Eq. (9) are in good agreement with the values estimated by Eq. (5) except for C_4mim[$OcSO_4$]. This is because that the Eq. (5) is valid mainly for ILs [$C_n$mim][NTf_2]. Indeed, the assumption to consider the quaternary ammonium cation as a ring system needs further confirmation.

Parameter (kJ·mol^{-1})	Value	Parameter (kJ·mol^{-1})	Value
ΔH_C	2.5	ΔH_P	4.1
ΔH_N	26.3	ΔH_S	-8.2
ΔH_O	23.6	ΔH_{CF_3}	-63.1
ΔH_B	23.0	ΔH_{ring}	27.1
ΔH_F	13.7		

Table 4. Parameters for predicting the enthalpy of vaporization of ILs at 298.15 K[25]

ILs	ρ / g·cm^{-3}	γ / mJ·m^{-2}	$\Delta_l g H_m^\theta$ / kJ·mol$^{-1,a}$	$\Delta_l g H_m^\theta$ / kJ·mol$^{-1,b}$
$[C_2mim][EtSO_4]$	1.2411[6]	45.44[6]	158.8	144.7
$[C_2mim][NTf_2]$	1.5187[6]	35.70[6]	132.9	139.3
$[C_4mim][NTf_2]$	1.4366[6]	32.80[6]	137.9	139.0
$[C_4mim][OcSO_4]$	1.0638[6]	26.71[6]	178.8	122.5
$[N_{4111}][NTf_2]$	1.3940[6]	32.46[6]	136.2	135.3
$[N_{8881}][NTf_2]$	1.1046[6]	27.93[6]	181.2	187.8
$[m_3opy][BF_4]$	1.0945[8]	36.51[8]	166.2	167.4

[a] data predicted from Eq.(9); [b] data estimated from Eq.(5)

Table 5. The values of the molar enthalpy of vaporization of ILs at 298.15 K

4.6 Conclusions

The physicochemical properties (molecular volume, molar volume, parachor, interstice volume, interstice fractions, thermal expansion coefficient, standard entropy, lattice energy and molar enthalpy of vaporization) of $[C_2mim][EtSO_4]$, $[C_4mim][OcSO_4]$ and $[C_2mim][NTf_2]$ were estimated by using their experimental data of density and surface tension. Based on the estimated data of the molecular volume and parachor, the physicochemical properties (density, surface tension and all of the properties mentioned above) for their homologue series $[C_nmim][EtSO_4]$, $[C_nmim][OcSO_4]$ and $[C_nmim][NTf_2]$ (n=1-6) were predicted.

We compared the values of molar enthalpy of vaporization for $[C_2mim][EtSO_4]$, $[C_4mim][OcSO_4]$, $[C_2mim][NTf_2]$, $[C_4mim][NTf_2]$, $[N_{4111}][NTf_2]$, $[N_{8881}][NTf_2]$ and $[m_3opy][BF_4]$, estimated by Kabo's empirical equation with those predicted by Verevkin's simple rule, and found that the values calculated in terms of the two approaches are in good agreement with each other. Hence, it is suggested that the molar enthalpy of vaporization of ILs could be estimated in terms of Verevkin's simple rule when the experimental data is not available.

4.6 Acknowledgement

The authors gratefully acknowledge the National Nature Science Foundation of China for providing financial support to carry out the studies under the Grant NSFC No 21073189, 21003068, 21071073.

4.7 References

[1] Tsunashima, K.; Sugiya, M. *Electrochem. Commun.*, 2007, 9: 2353
[2] Seki, S.; Kobayashi, Y.; Miyashiro, H.; Ohno, Y.; Usami, A.; Mita, Y.; Watanabe, M.; Terada, N. *Chem. Commun.*, 2006, 544
[3] Itoh, H.; Naka, K.; Chujo, Y. *J. Am. Chem. Soc.*, 2004, 126: 3026
[4] Du, Z.; Yu, Y. L.; Wang, J. H. *Chem. Eur. J.*, 2007, 13: 2130
[5] Endres, F.; Abedin, S. Z. E. *Phys. Chem. Chem. Phys.*, 2006, 8: 2101
[6] Wandschneider, A.; Lehmann, J. K.; Heintz, A. *J. Chem. Eng. Data*, 2008, 53: 596
[7] Bandres, I.; Giner, B.; Artigas, H.; Lafuente, C.; Royo, F. M. *J. Chem. Eng. Data*, 2009, 54: 236
[8] Sun, J.; Forsyth, M.; MacFarlane, D. R. *J. Phys. Chem. B*, 1998, 102: 8858
[9] Tokuda, H.; Hayamizu, K.; Ishii, K.; Susan, M. A. B. H.; Watanabe, M. *J. Phys. Chem. B*, 2004, 108: 16593
[10] Tokuda, H.; Ishii, K.; Susan, M. A. B. H.; Tsuzuki, S.; Hayamizu, K.; Watanabe, M. *J. Phys. Chem. B*, 2006, 110: 2833
[11] Bandrés, I.; Giner, B.; Artigas, H.; Royo, F. M.; Lafuente, C. *J. Phys. Chem. B*, 2008, 112: 3077
[12] Tong, J.; Liu, Q. S.; Guan, W.; Yang, J. Z. *J. Phys. Chem. B*, 2007, 111: 3197
[13] Tong, J.; Liu, Q. S.; Zhang, P.; Yang, J. Z. *J. Chem. Eng. Data*, 2007, 52: 1497
[14] Fang, D. W.; Guan, W.; Tong, J.; Wang, Z. W.; Yang, J. Z. *J. Phys. Chem. B*, 2008, 112: 7499
[15] Tong, J.; Liu, Q. S.; Xu, W. G.; Fang, D. W.; Yang, J. Z. *J. Phys. Chem. B*, 2008, 112: 4381
[16] Fernández, A.; Torrecilla, J. S.; García, J.; Rodríguez, F. *J. Chem. Eng. Data*, 2007, 52: 1979
[17] Fernández, A.; García, J.; Torrecilla, J. S.; Oliet, M.; Rodríguez, F. *J. Chem. Eng. Data*, 2008, 53: 1518
[18] Glasser, L. *Thermochim. Acta*, 2004, 421: 87
[19] Troncoso, J.; Cerdeirina, C. A.; Sanmamed, Y. A.; Romani, L.; Rebelo, L. P. N. *J. Chem. Eng. Data*, 2006, 51: 1856
[20] Hasse, B.; Lehmann, J.; Assenbaum, D.; Wasserscheid, P.; Leipertz, A.; Froba, A. P. *J. Chem. Eng. Data*, 2009, 54: 2576
[21] Deetlefs, M.; Seddon, K. R.; Shara, M. *Phys. Chem. Chem. Phys.*, 2006, 8: 642
[22] Zaitsau, D. H.; Kabo, G. J.; Strechan, A. A.; Paulechka, Y. U.; Tschersich, A.; Verevkin, S. P.; Heintz, A. *J. Phys. Chem. A*, 2006, 110: 7303.
[23] Yang, J. Z.; Lu, X. M.; Gui, J. S.; Xu, W. G. *Green Chem.*, 2004, 6: 541
[24] Zhang, Q. G.; Yang, J. Z.; Lu, X. M.; Gui, J. S.; Huang, M. *Fluid Phase Equilib.*, 2004, 226: 207
[25] Verevkin, S. P. *Angew. Chem. Int. Edit.*, 2008, 47: 5071

Ionic Liquids: Theory, Properties, New Approaches
Edited by Prof. Alexander Kokorin

ISBN 978-953-307-349-1
Hard cover, 738 pages
Publisher InTech
Published online 28, February, 2011
Published in print edition February, 2011

Ionic Liquids (ILs) are one of the most interesting and rapidly developing areas of modern physical chemistry, technologies and engineering. This book, consisting of 29 chapters gathered in 4 sections, reviews in detail and compiles information about some important physical-chemical properties of ILs and new practical approaches. This is the first book of a series of forthcoming publications on this field by this publisher. The first volume covers some aspects of synthesis, isolation, production, modification, the analysis methods and modeling to reveal the structures and properties of some room temperature ILs, as well as their new possible applications. The book will be of help to chemists, physicists, biologists, technologists and other experts in a variety of disciplines, both academic and industrial, as well as to students and PhD students. It may help to promote the progress in ILs development also.

InTech Europe
University Campus STeP Ri
Slavka Krautzeka 83/A
51000 Rijeka, Croatia
Phone: +385 (51) 770 447
Fax: +385 (51) 686 166
www.intechopen.com

InTech China
Unit 405, Office Block, Hotel Equatorial Shanghai
No.65, Yan An Road (West), Shanghai, 200040, China
中国上海市延安西路65号上海国际贵都大饭店办公楼405单元
Phone: +86-21-62489820
Fax: +86-21-62489821

IntechOpen